materials

MDPI

Review

Ion-Imprinted Polymers: Synthesis, Characterization, and Adsorption of Radionuclides

Vipul Vilas Kusumkar [1,*], Michal Galamboš [1,*], Eva Viglašová [1], Martin Daňo [2] and Jana Šmelková [3]

[1] Department of Nuclear Chemistry, Faculty of Natural Sciences, Comenius University in Bratislava, Mlynska dolina Ilkovicova 6, 842 15 Bratislava, Slovakia; eva.viglasova@uniba.sk
[2] Department of Nuclear Chemistry, Faculty of Nuclear Sciences and Physical Engineering, Czech Technical University in Prague, Brehová 7, 115 19 Prague, Czech Republic; martin.dano@fjfi.cvut.cz
[3] Department of Administrative Law and Environmental Law, Faculty of Law, Comenius University in Bratislava, Safarikovo namestie 6, 810 00 Bratislava, Slovakia; jana.smelkova@uniba.sk
* Correspondence: kusumkar1@uniba.sk (V.V.K.); michal.galambos@uniba.sk (M.G.); Tel.: +421-2-9014-9351 (M.G.)

Abstract: Growing concern over the hazardous effect of radionuclides on the environment is driving research on mitigation and deposition strategies for radioactive waste management. Currently, there are many techniques used for radionuclides separation from the environment such as ion exchange, solvent extraction, chemical precipitation and adsorption. Adsorbents are the leading area of research and many useful materials are being discovered in this category of radionuclide ion separation. The adsorption technologies lack the ability of selective removal of metal ions from solution. This drawback is eliminated by the use of ion-imprinted polymers, these materials having targeted binding sites for specific ions in the media. In this review article, we present recently published literature about the use of ion-imprinted polymers for the adsorption of 10 important hazardous radionuclides—U, Th, Cs, Sr, Ce, Tc, La, Cr, Ni, Co—found in the nuclear fuel cycle.

Keywords: ion-imprinted polymers; radioactive waste; radionuclides; adsorption; separation

Citation: Kusumkar, V.V.; Galamboš, M.; Viglašová, E.; Daňo, M.; Šmelková, J. Ion-Imprinted Polymers: Synthesis, Characterization, and Adsorption of Radionuclides. *Materials* **2021**, *14*, 1083. https://doi.org/10.3390/ma14051083

Academic Editors: Lionel Limousy and Antonio Gil Bravo

Received: 28 December 2020
Accepted: 22 February 2021
Published: 26 February 2021

1. Introduction

Spent nuclear fuel (SNF) and high-level radioactive waste (HLRW) are generated during nuclear power reactor operation and decommissioning of nuclear facilities, respectively. There are 62 different radionuclides (RNs) formed from ^{235}U fission, which due to their instability, are subject to radioactive transformation. About 200 different radioisotopes are observed during the nuclear reactor operation, mainly in the core. Nuclear power plants around the world are the major producers of SNF and HLRW. Situated on the territory of the Slovak republic are in Jaslovské Bohunice (Bohunice 4 and 3—reactor units in operation; Bohunice 2, 1 and A1—in the decommissioning process) and Mochovce (Mochovce 1 and 2—reactor units in operation; Mochovce 3 and 4—reactors units under construction).

Slovak legislation on SNF and radioactive waste (RW) management fully corresponds to international legislation and regulations. Requirements for the management of SNF and RW have been regulated in the Act No. 541/2004 Collection on the peaceful use of nuclear energy (Atomic Act) and in its implementing regulation and the Act No. 308/2018 Collection on the National Nuclear Fund and amending the Atomic Act. The Atomic Act defines RW as any unusable material in gaseous, liquid, or solid form, which cannot be released into the environment due to the content of RNs or the level of RN contamination. Details on the requirements for the management of nuclear materials, RW, and SNF are also defined by the Decree of the Nuclear Regulatory Authority of the Slovak Republic No. 30/2012 Collection. It is assumed that the individual units of nuclear power plants in Slovakia will produce 2500 tons of SNF and 3700 tons of HLRW during their operation period. Produced SNF can be considered either as a usable source of energy and RNs and can be reprocessed or can be destined for final disposal if it is considered as RW.

By ^{235}U fission two main groups of RNs are created:

(1) *Fission products (FPs)*: formed by the fission of fuel nuclei by neutrons. These are highly active RNs; whose half-life ranges from a few seconds to thousands of years:
- volatile substances (^{99}Tc, ^{103,106}Ru, ^{131,133,135}I, ^{134,135,137}Cs, ...),
- non-volatile substances (^{90}Sr, ^{140}La, ^{141,144}Ce, ...),
- noble gases (^{85}Kr, ^{131,133,135}Xe), tritium (^{3}H).

(2) *Activation products (APs)*: formed by the interactions of neutrons with inactive nuclides of the coolant, moderator, or reactor construction materials, respectively. By activating the reactor construction materials, the following main activation corrosion and erosion products are formed:
- steel: ^{51}Cr, ^{54}Mn, ^{60}Co, ^{63}Ni, ^{59}Fe, ^{93}Mo, ^{94}Nb, ^{108m,110m}Ag, ^{124,125}Sb, ^{152}Eu, ^{166m}Ho,
- concrete: ^{36}Cl, ^{41}Ca, ^{46}Sc, ^{51}Cr, ^{59}Fe, ^{59}, ^{63}Ni, ^{60}Co, ^{65}Zn, ^{85}Sr, ^{124}Sb, ^{131}Cs, ^{152,154,155}Eu, ^{160}Tb, ^{181}Hf, ^{182}Ta.

The gradual capture of neutrons by fuel nuclei and their subsequent radioactive transformations produce transuranic elements. The most commonly used source nuclides of transuranic elements are ^{238}U, ^{237,239}Np, ^{238,242}Pu, ^{241,243}Am, ^{242,244}Cm. The RNs with the half-life longer than >200,000 years, such as: ^{79}Se, ^{93}Zr, ^{99}Tc, ^{107}Pd, ^{126}Sn, ^{129}I, ^{135}Cs which are difficult to measure, play significant roles in the separation processes. However, there are also other problematically detected RNs with shorter half-life < 200,000 are i.e., ^{59,63}Ni, ^{79}Sc, ^{146}Sm, and actinide ^{236}U.

Uranium is the most significant metal for energy production and also the primary waste generated from nuclear reactor operation. Uranium is known for its toxicity, apart from the fact that ingestion of uranium can damage the liver and cause acute renal failure in humans [1]. The uranyl ion (UO_2^+) occurs in oxidation state 6+ and is the most stable form of uranium in aqueous solution [2–4]. According to safety regulations, uranium consumption in drinking water should be less than 0.015 mg/L [5]. *Thorium* is a metallic element of the actinides. For energy generation, thorium is a better choice than uranium due to its abundance on Earth, and the relatively less radioactive waste generated from its operation in a nuclear reactor. More than 99.99% of natural thorium is ^{232}Th, the rest being represented by ^{230}Th and ^{228}Th. Thorium metal occurs naturally in the environment. The increasing release of these metals has spiked due to mining activity, e.g., milling, and processing operation, coal production, and phosphate production for fertilizers. Besides its attractive properties for nuclear energy generation, it is toxic element for human health, as a potentially carcinogenic substance. Thorium exposure is primarily due to inhalation, intravenous injection, ingestion and absorption through the skin [6]. The dispersion of thorium in the environment, mainly in water bodies, creates great concern to humans and ecological life forms [7,8]. *Cesium-137* and *Strontium-90* are isotopes produced during a nuclear power plant's operation by ^{235}U fission and are the most harmful RNs due to their strong beta emission properties and long half-life (30 years, and 29 years, respectively). The nuclear accidents in Chernobyl and the Fukushima Daiichi released large amounts of cesium isotopes (^{134}Cs, ^{137}Cs) into the surroundings [9]. These radionuclides are highly soluble and mobile in water. ^{90}Sr can accumulate in human organs, mostly in the liver, lungs, and kidneys of animals, and causes diseases and damage [10,11]. *Cerium-144* (half-life 284.91 days) is formed by the fission of uranium and accumulates in the human body leading to acute myocardial infarction, leukemia, and imbalance in blood biochemistry. It also causes a toxic effect damaging the cell membranes in marine life, consequently damaging the nervous system and reproduction system in organisms [12,13]. The nuclear power generation from uranium generates a significant amount (≈6.05%) of *Technetium-99*, which as a FP is highly toxic due to its high mobility in water and a half-life of 2.11×10^5 years [14]. *Lanthanum-140* (half-life 1.68 days) occurs as a FP of uranium; it has no biological role and is considered an environmental threat due to its radioactivity [15]. *Chromium-51* (half-life 27.70 days) is an AP and can be used as a radioactive tracer in isotope dilution analysis. Chromium is needed in trace amounts for the proper functioning of the

human body, but its excess can cause carcinogenic effects [16]. *Nickel-59, 63* are isotopes generated in the nuclear reactor as APs [17]. ^{59}Ni and ^{63}Ni have a half-life of 76,000 and 101.2 years, respectively [18]. Nickel is responsible for various health effects on humans, depending on the route of exposure and dosage. It can cause cardiovascular diseases, skin diseases, nose and lung cancer [19]. *Cobalt-60* is generated in the nuclear power plant. ^{60}Co is the source of high gamma radiation and has a half-life of 5.27 years. The presence of cobalt in the environment, considering its radioactivity, can cause detrimental effects on ecology and human health [20].

For the mitigation of radionuclides' environmental impact, various methods have been used to date such as phytoremediation [21], ion-exchange [22], chemical precipitation [23], solvent extraction [24], reverse osmosis [25], electrochemical purification [26], membrane separation [27] and adsorption [28]. The adsorption method is the most reliable method for toxic radionuclide removal and has been widely used. Numerous materials can be utilized for adsorption purposes such as inorganic sorbents [29], oxides [29–31], carbon materials [32], organic-inorganic hybrid materials [33], metal-organic frameworks [34] and porous organic polymers [35]. Although the adsorbents used in nuclear waste management, e.g., ion exchangers and inorganic materials are constantly improving over the time in their structural, physical, and chemical aspects [36], these materials also have disadvantages, e.g., rapid saturation, etc.

The Department of Nuclear Chemistry, Faculty of Natural Sciences, Comenius University in Bratislava, has long been dedicated to the development and research on various highly selective and radiation-stable sorbents, which are used:

- as a component in a multibarrier system for the safe storage and final disposal of SNFs and RWs, respectively,
- as a separation component for RN isolation from RN mixtures, mainly for further use, or in radiochemical analysis for target radionuclide separation and subsequent qualitative and quantitative determination.

Ion-imprinted polymers (IIPs) can solve this issue and are widely used for in radionuclide adsorption or removal processes [37]. IIPs are sorbents with various application possibilities, e.g., extraction, filtration, solid and liquid media purification [38]. These materials are crosslinked polymers with pores and binding sites for the targeted ions and negatively or positively charged molecules [39]. IIPs are generally prepared from a reaction mixture composed of a functional monomer, a crosslinker, an initiator and a template [40]. Imprinting of the template ions in a polymer matrix can be achieved by using different strategies and are discussed further in detail. IIPs are developed in a similar way to imitate key and lock mechanisms (Figure 1) for recognition and removal of the targeted ions. Thus, IIPs offer excellent selectivity and specific affinity for a given ion. Contaminants present at low concentrations can be removed selectively by IIPs, which was not effectively achieved before by other methods [41]. IIPs are similar to molecularly imprinted polymers (MIPs) which are developed to imitate the interactions between enzymes and antibodies. The difference between IIPs and MIPs lies in the type of recognition substance which can be ions or molecules.

MIP and IIP preparation differ in the type of interaction between the monomers or ligands (MIPs) and ions (IIPs), i.e., covalent or noncovalent interactions. The covalent molecular imprinting technique method developed by Wulff et al. [42], involves reversible covalent binding between monomers and the templates. This approach provides greater stability and consistent recognition sites compared to the non-covalent approach. In the non-covalent method, the non-covalent bonds such as H-bonds, ionic bonds, van der Waals interactions, etc. are used by monomers to self-assemble around the template. The template is then removed from the material after polymerization. Mosbach et al. [43] developed the non-covalent method, which is an effective way to form cavities with the template's shape and charge memory effects, responsible for the selective recognition of analytes. The non-covalent method is easy to use and has the option to choose from a range of different monomers. IIPs exhibit similar virtues as MIPs, the only difference being the

specific recognition of inorganic ions after the imprinting process [44,45]. The first IIP preparation was achieved using poly(vinyl pyridine) crosslinked with 1,4-dibromobutane in the presence of metal ions [46]. Saunders et al. [47] used 2-chloroacrylic acid and ethylene glycol dimethacrylate (EGDMA) with a uranyl ion-imprinted co-polymer after removal of the template. This material selectively extracts uranium from dilute aqueous solutions. He et al. [48] synthesized a new functional monomer—*N*-(*o*-carboxyphenyl) maleamic acid (CPMA)—for Th(IV) ion separation. This adsorbent was made of a silica gel surface coating with a thin IIP layer.

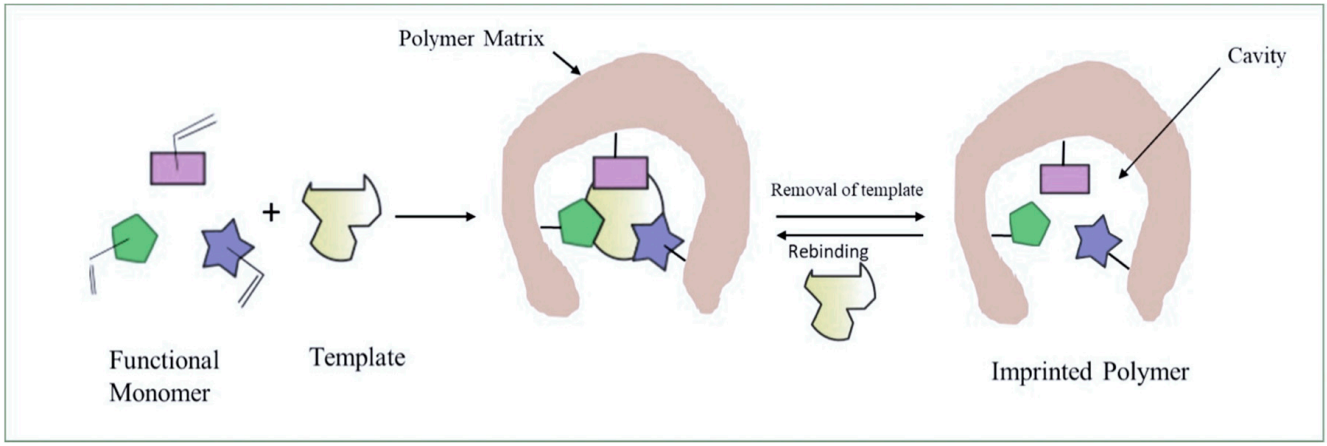

Figure 1. Schematic presentation of the procedure for the preparation of imprinted polymers.

A few reviews can be found on IIP technologies for adsorption/removal of a larger group of metal ions such as a review on IIPs for removing inorganic pollutants by Mafu et al. [49]. Further, Hande et al. [50] described synthesis methodologies for several applications, and recent advances in imprinted polymers can be found in the publication of Branger et al. [51]. A review article on imprinted polymers developed from halloysite nanotubes for environmental pollutant removal can be found [52] and more discoveries were published in [53,54]. To the best of our knowledge, there is no specific review describing the use of IIPs for specific radionuclides. Our study's focus is to provide an update on the theoretical background about the adsorption of ten important radionuclides—U, Th, Cs, Sr, Ce, Tc, La, Cr, Ni, Co—by IIPs and its fundamental aspects. In the following sections, the fundamentals of IIPs and IIPs' adsorption processes of various radionuclides are discussed.

2. Fundamentals of IIPs Synthesis for Radionuclides Adsorption

The synthesis of IIPs is commonly carried out in the following way: First, monomers containing functional groups are mixed with template ions, whereupon the monomers self-assemble around the ions. Second, a crosslinker is used to polymerize the monomers by using a photo- or thermal polymerization technique. Third, template ions are removed from the polymers, consequently generating specific binding sites that can capture target ionic species [55]. IIPs shows excellent ion selectivity due to their recognizable binding sites for a particular ion's size and charge. The adsorption capacity of the IIPs is influenced by certain factors, such as their ligands' ability to bind with metal ions, ionic charge, the size of ions, and the electronic configuration of the metals such as coordination number or oxidation states [56,57]. The IIPs are stable against pH, temperature, and pressure which is almost impossible to achieve in natural molecular recognition systems [58].

2.1. Principles and Basic Components for the Synthesis of IIPs

One of the most crucial criteria for the effective binding and selectivity of the metal ion to the imprinted material is the interaction of the functional groups of monomers with

the template [59]. The template interaction depends upon the type of bonding present with monomers. Two approaches, as mentioned earlier, are used: the covalent approach and the non-covalent approach. The IIPs are developed using a template, functional monomers, crosslinkers, porogens, and initiators. The ratio and the selection of these components are essential for better selectivity and binding capacity and affect the ultimate physical and chemical properties of the IIPs.

2.1.1. Templates

The selection of templates is a crucial requirement for IIP development. The templates' chemical and physical properties are analyzed for their selection. The basic requirements for choosing a template are as follows:

- The template should be inert, it should not affect the cross-linking and polymerization of the monomer, e.g., the functional moieties shouldn't interfere with the polymerization by acting as inhibitors or reacting with the monomer.
- The template should be cost-effective.
- The template should be stable at the polymerization or crosslinking temperature or exposure to UV radiation.

2.1.2. Monomers and Crosslinkers

In order to prepare recognition sites in a polymer matrix monomer should have functional groups that will bind with the analytes. Monomer selection is an important factor for the design of IIPs. To prepare imprinted polymers a free radical polymerization (FRP) method is used since it is easy to execute and offers a wide range of monomer selection. Generally, in radical polymerization (RP) of IIPs vinyl monomers are used, e.g., methacrylic acid [60], acrylamide [61], styrene [62], 4-vinylpyridine [63], etc. The monomers are crosslinked using di-, tri-, or tetrafunctional vinylated crosslinkers. Crosslinkers are useful for improving the mechanical properties of the material such as strength and tolerance to the solvent and different pH values. They also help the morphology of the material and adjusting the monomer–crosslinker ratio affects the materials' porosity. Commonly used crosslinkers for free radical polymerization are ethylene glycol dimethacrylate (EGDMA) [64], divinylbenzene (DVB) [65], or trimethylolpropane trimethacrylate (TRIM) [66]. The ratio of the template to monomer is crucial. The compatibility ratio for the adsorption of UO_2^+ ion was found to be 1:4 template to monomer, and exceeding the ratio will cause reduced interaction with the template [67]. The abovementioned monomers' binding capacity is relatively weaker; they carry a single functionality for interaction. The dependence on a metal ion's characteristics such as shape, oxidation, and chemical structure and surroundings play an important role in its effective binding [68]. To improve the binding performance of the materials, various ligands were prepared for effective binding with selective ions. Fasihi et al. [69] synthesized a 1-hydroxy-2-(prop-2′-enyl)-9,10-anthraquinone ligand to prepare uranyl IIPs. Zulfikar et al. [70] prepared 5,7-dichloroquinoline-8-ol and 4-vinylpyridine-based IIPs for the adsorption of yttrium. Macromolecular monomers such as chitosan and, sodium alginate are also widely used to remove radionuclides from the environment [71,72]. Chitosan has NH_2 and -OH groups that will donate to the metals and be useful for chelation and crosslinking [73]. Sodium alginate contains -COOH and -OH groups, which helps provide the necessary binding sites for the preparation of IIPs [74].

2.1.3. Porogens (Solvents)

The purpose of the solvent in the polymerization is to solubilize the components of the reaction mixture such as monomers, templates, and crosslinkers. It helps in pore formation in a material, which improves the material's adsorption properties [75]. The solvent choice depends on the reaction system interactions. In the case the system consists of organic molecules that contain hydrogen atoms, for that purpose nonpolar solvents such as toluene can be used, and for polar systems, water or other polar solvents have been used [76].

2.1.4. Initiators

The initiator is responsible for the activation of free radical polymerization in monomers. The initiator selection depends on the template ion's stability and electrostatic interactions with the monomers, mainly for complex formation. If initiators are thermally activated, thermal stability of the template is also required. If the monomers form a complex with the template ions by hydrogen bond formation, then it is not appropriate to use a thermal method. However, a photochemically activated initiator is more reliable for using such a low stability template and its interactions. The initiator concentration is directly related to the generation of radicals in the system, which increases the particle size of the IIPs [77]. Some of the initiators used are shown in Figure 2.

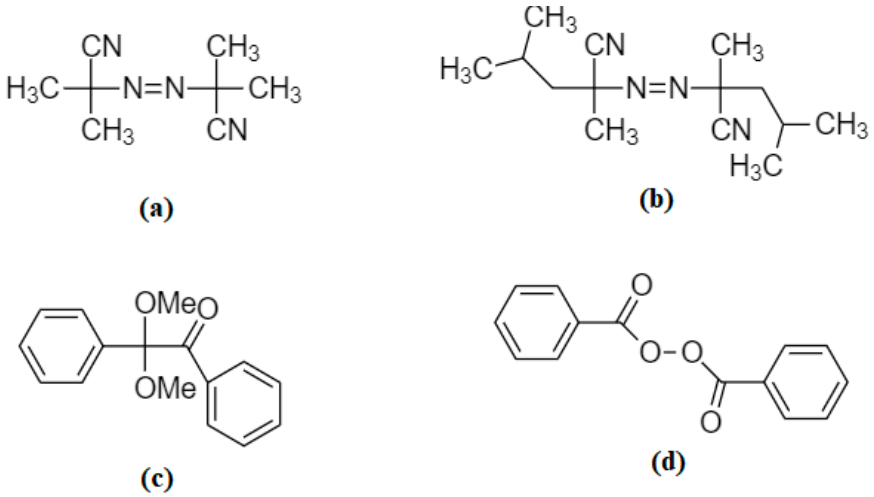

Figure 2. Commonly used initiators: (**a**) azobisisobutyronitrile (AIBN), (**b**) azobisdimethylvaleronitrile (ABDV), (**c**) benzildimethyl acetal, (**d**) benzoyl peroxide (BPO).

2.2. Imprinting Strategy for the IIPs Synthesis

The preparation of IIPs can be performed in several ways using multiple preparation methods. In this section, the most commonly used type of polymerization or imprinting strategies are described. The simplest method for IIP synthesis is radical polymerization (RP). Radical polymerization can be divided into bulk polymerization [78], emulsion polymerization [79], solution polymerization [80], precipitation polymerization [81] and reversible addition-fragmentation techniques (RAFT) polymerization [82]. In the living free radical polymerization method (for e.g., RAFT) the desired polymer morphologies can be achieved [83]. RP also provides significantly faster polymerization rates compared to the condensation polymerization method. The system in RP contains the monomer, initiator and crosslinker, if required. Another common method for making crosslinked structures is the condensation method, which includes sol-gel and co-condensation polymerization. Chitosan is a functional group-carrying polymer with -NH_2 and -OH groups which can be modified with other compounds, in order to form a dendritic structure or crosslinked networks. For the preparation of crosslinked structures chitosan can be crosslinked with various difunctional molecules such as glutaraldehyde [84], epichlorohydrin, etc. In another study, Gao et al. [85] used 3-glycidoxypropyltrimethoxysilane (GPTMS) for crosslinking chitosan or silane coupling agents. Imprinting metal ions on the materials' surface solves certain drawbacks associated with the use of IIPs, such as poor mass transfer and binding kinetics. The surface of imprinted polymers can improve the selectivity and specificity of the materials' surface, which is not found in general IIPs [86].

3. Adsorption Performance of IIPs

3.1. Quantities for Measuring Adsorption Performance of IIPs

IIPs are known for their selectivity towards the analytes, and IIPs' adsorption performance can be studied with respect to a non-imprinted polymer (NIP) which is synthesized using the same procedure but without the template ion. Two different equations are used for calculation, one is the % *removal* and the other one is equilibrium adsorbate concentration. The % *removal* represents the approximate value of the adsorption performance and it is shown in Equation (1):

$$\% \ removal = 100 \times (C_0 - C_e)/C_0 \quad (1)$$

where C_o (mg/L) is the initial adsorbate concentration and C_e (mg/L) equilibrium concentration in the solution. The equation for the adsorption performance (Equation (2)) is derived from the expression of the equilibrium concentration of the adsorbate Q_e (mg/g) at the amount of adsorbate adsorbed at the equilibrium [87]:

$$Q_e = V \times (C_0 - C_e)/m \quad (2)$$

where m (g) is the dry mass of the used adsorbent; V (L) is the volume of the adsorbate solution.

3.2. Adsorption Isotherm

Adsorption isotherms can be defined by the relationship between the amount of adsorbate adsorbed on the adsorbent at equilibrium and the adsorbate's concentration at equilibrium in the solution. This relationship is determined by plotting Q_e against C_e. The Data modeling is achieved using different models such as Langmuir, Freundlich, etc. [88]. To understand the binding capacity of IIPs, the graphs are compared with non-imprinted polymers (NIP). The Langmuir model only deals with a measurable number of the binding sites on an IIP's surface and is also limited to monolayer adsorption [89]. In IIPs, the Langmuir model was used based on two assumptions: the adsorbed molecules will not interact, and after the analyte occupies the available binding sites, no further adsorption will be possible [90]. A linear form of the Langmuir Equation (3) is presented as follows:

$$1/q_e = (1/q_{max} \times b \times C_e) + (1/n) \times log\ C_e \quad (3)$$

where q_e is the equilibrium of the amount of uranyl ions adsorbed on the adsorbent (μmol/g), q_{max} is the maximum adsorption capacity (μmol/g), C_e is the equilibrium concentration of uranyl ions in the solution (μmol/L), b is the Langmuir constant (L/μmol). q_{max} and b are the Langmuir constants, which can be calculated from the intercept and slope of the linear plot based on $1/q_e$ versus $1/C_e$.

The Freundlich model can be applied on heterogeneous surfaces with the extension of multilayer adsorption [58]. Similarly, the linear Freundlich isotherm equation can be presented as follows:

$$log\ q_e = log\ K_f + (1/n) \times log\ C_e \quad (4)$$

where the K_f denotes the Freundlich isotherm constant and $1/n$ is the heterogeneity factor.

The Langmuir and Freundlich isotherms are commonly used isotherms in order to describe sorption experiments. However, other different isotherms models are also studied instead of the Langmuir or Freundlich isotherms. To investigate the adsorption of Cs^+ ion on two different RAFT IIPs, Meng et al. [91] applied three isotherm models: Freundlich, Langmuir, and Redlich-Peterson. In this study, the Redlich-Peterson model was found to be more relevant to the experimental data, based on correlation coefficient values. In another study, apart from the Langmuir and Freundlich isotherm model, the Dubinin-Radushkevitch (D-R) model was successfully applied and gave a better fit for the adsorption of uranium in comparison with previous ones. Sadeghi et al. [87] applied both Freundlich and Langmuir models for finding the binding capacity of an IIP, and

the experimental results showed that Langmuir isotherm better corresponded with the experimental data, based on correlation factors.

3.3. Influence of pH onto Radionuclides Adsorption by IIPs

Changes in the solution acidity or basicity affect the concentration of H^+ ions in a solution. At lower pH values, the self-assembly process reduces the choice of metal ions over H^+ ions. Thus, a higher pH value favors complex formation. On the other hand, the pH also determines the material's surface properties and protonation level, which directly control the electrostatic interactions with the interacting species. In the study carried out by Sadeghi et al. [92], experiments performed in a strongly acidic medium revealed that uranyl ions' removal capacity decreased due to the protonation of the amine group in the IIP adsorbent. Monier et al. [69] found that acidic conditions bind with the active amidoxime sites in the adsorbent, which leads to a lower adsorption capacity, whereas at values up to pH~5, the UO_2^+ ion removal efficiency is increased. In the range of pH values higher than pH~5, uranyl ions are precipitated in the form of UO_2OH^+ and $UO_2(OH)_2$. These hydrolyzed forms caused a decrease in the adsorption performance [72]. pH~6 was found to be optimal for strontium and the increase of pH caused less the adsorption efficiency due to hydrolyzed ion species [93]. The lower pH value forms carboxylate [79] and amino groups [94] in IIPs, which leads to a decrease in adsorption capacity. A similar adsorption behavior was found in the case of other RNs, e.g., cobalt [95] and technetium [96].

3.4. Influence of Dosage and Concentration onto Radionuclides Adsorption by IIPs

Except for the pH, other essential factors for optimal adsorption are the adsorbent dosage and adsorbate concentration. Tawengna et al. showed an increase in extraction efficiency from 47 to 80% and 35 to 62% with an increase in the amount of adsorbent from 10 to 50 mg for magnetic IIPs and NIPs, respectively. This increased extraction efficiency is explained due to the rise in adsorption sites and surface area for analyte adsorption. The initial concentration of the uranyl ion solution was varied from 0.5 and 8 mg/L using 50 mg of IIP adsorbent, and the experiments showed that the saturation point was reached at 2 mg/L of initial concentration. Maximum adsorption capacities of 1.04 ± 0.03 and 0.95 ± 0.02 mg/g were observed for magnetic IIPs and NIPs, respectively. This adsorption capacity is increased due to the increased strength of the transfer force and the mass transfer [90]. In another study, an adsorbent dosage in the range of 10–100 mg was applied for uranyl ion extraction from an aqueous solution. The study proved that the maximum extraction efficiency was achieved at 50 mg, and a further increase of adsorbent dose did not improve the performance of the adsorbent [97].

4. Application of IIPs for Radionuclide Removal

4.1. Uranium

Uranium occurs in Nature mainly in the forms of 4+ and 6+ oxidation states. The most common uranium form is uranium oxide, the uranyl cation UO_2^+, and it is the most generally used template for IIP production [98]. Ahmadi et al. [99] prepared uranyl ion-imprinted polymers applying the following steps: (a) formation of a uranyl binary complex with N,N-ethylenebis(pyridoxylideneiminato); (b) synthesis of a $[UO_2(pyr_2en)DMSO]Cl_2$ ternary complex with 4-vinylpyridine, and (c) polymerization of the ternary complex with styrene. The prepared polymer showed excellent selectivity and adsorption performance towards uranyl ion compared to other heavy metals. The use of quinoline-8-ol functionalized by 3-aminopropyltrimethoxysilane-modified silica nanoparticles (HQ-APTMS-SI) is mainly used for imprinted polymer nanosphere preparation. This was developed and studied primarily for selective uranyl ion capture for the decontamination of nuclear power plant effluents by Milia et al. [100]. This method is schematically shown in Figure 3. The interpenetration networks of crosslinked hydrogel uranyl IIPs were prepared from chitosan and polyvinyl alcohol with the difunctional crosslinker ethylene glycol diglycidyl ether developed by Liu et al. [101]. Zhou et al. [102] prepared magnetite uranyl IIP from

chitosan crosslinked with glutaraldehyde. Sadeghi et al. [92] prepared uranyl-imprinted silica-coated magnetic nanoparticles. The resultant polymer is a base platform for the development of functionalized nanomaterials for imprinted materials.

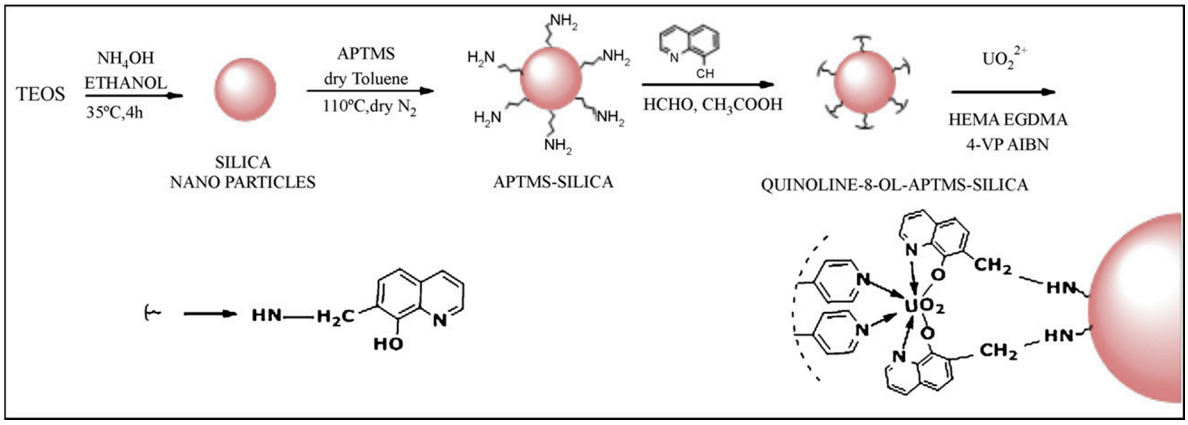

Figure 3. Schematic presentation of uranyl ion-imprinted nanospheres preparation from silica nanoparticles. Reprinted with permission from ref. [100], copyright 2011, Milja et al.

Pakade et al. [98] prepared a novel uranyl ion-imprinted polymer from 1-(prop-2-en-1-yl)-4-(pyridin-2-ylmethyl) piperazine and methacrylic acid, crosslinked by using EGDMA. Monier et al. [76] prepared a cellulose-based imprinted polymer for uranyl ion removal. The cellulose was modified with salicylaldehyde, which was crosslinked in the presence of uranyl template with formaldehyde. Zhang et al. [99] developed a typical uranyl ion-imprinted polymer using free radical polymerization from the vinyl monomers 2,4-dioxopentan-3-yl methacrylate and the crosslinker EGDMA in the presence of uranyl ion as a template. Tavengwa et al. [100] developed the new uranyl ion magnetic imprinted polymer embedded with γ-methacryloxypropyltrimethoxysilane (γ-MPS). The silane monomer not only helps the polymer, but also helps to stabilize the Fe_3O_4 nanoparticles. In another study, Monier et al. [69] prepared amidoximated modified sodium alginate (Na-Alg) for the development of U-IIPs using glutaraldehyde as a crosslinker. The same authors prepared uranyl ion chelating microsphere using salicylaldehyde and *p*-aminostyrene (Schiff base), mainly used for the complex formation with UO_2^+ ion and later used as crosslinked with divinylbenzene (DVB) [101]. Tavengwa et al. [85] prepared oleic acid-modified magnetic nanoparticles coated with the imprinted polymer by a precipitation-polymerization method. Meng et al. [57] synthesized amine-functionalized silica, later modified with acrolyl chloride. The prepared vinylated silica was crosslinked with EGDMA and MAA in the presence of uranyl ion. Tavengwa et al. [102] prepared 3 γ-(methacryloxy)propyltrimethoxysilane (γ-MPS) coated magnetic uranyl ion-imprinted polymer in the form of nanocomposite beads using salicylaldoxime (SALO) as 4-vinylpyridine (4-VP) monomer by a bulk polymerization technique. Yang et al. [103] developed a uranyl ion mesoporous silica functionalized using diethylphosphatoethyltriethoxysilane (DPTES) and poly(ethylene glycol)-block-poly(propylene glycol)-block-poly-(ethylene glycol) copolymer (P123). These materials have shown excellent radioresistance stability and high regeneration capacity in acidic and radioactive media and are shown in Figure 4.

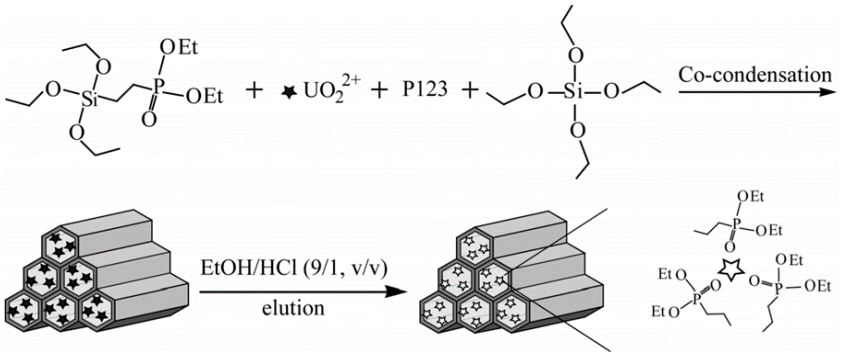

Figure 4. Schematic presentation of the preparation of ion-imprinted mesoporous silica. Reprinted with permission from ref. [103], copyright 2017, Yang et al.

Zhu et al. [104] used an interesting approach for generating ion-imprinted hierarchical porous carbon materials by using a hyper-accumulation method. The plant *Suaeda glauca* was used for this purpose to hyperaccumulate uranium ion from aqueous solution, later the material was kept for carbonization, mainly after successful ion removal from the carbonized material. The material was then used for further investigations. In another study, Wang et al. [105] prepared highly selective and sensitive uranium sensors. The imprinted polymer was produced using the sol-gel method where isophthalaldehyde-tertrapyrrole (IPTP) was used as a ligand for the synthesis, and α-methacrylic acid was used as a functional monomer. The uranyl ion template was used for the preparation, whereas the polymer was coated on a carbon paste electrode (CPE) (Figure 5).

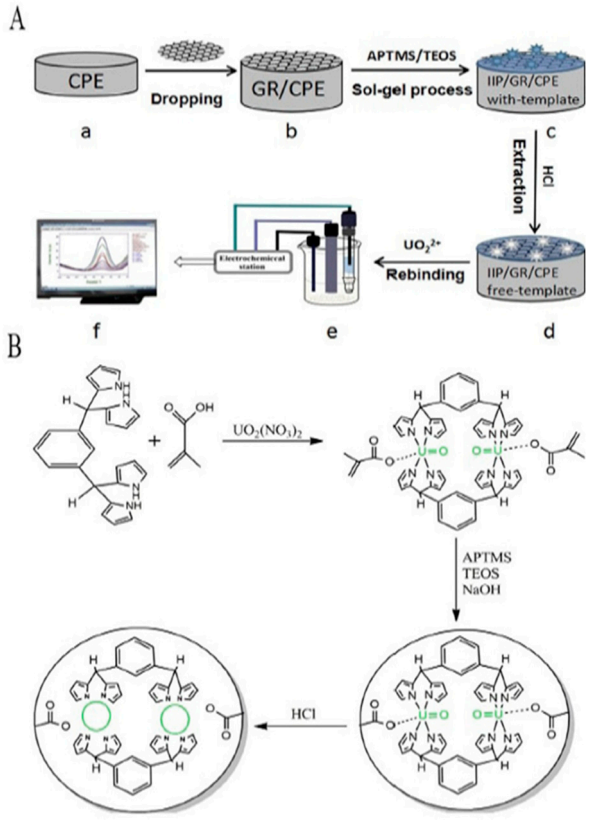

Figure 5. Schematic presentation for the preparation of a uranyl ion-imprinted sensor: (A) surface imprinting polymerization of the U-IIP on the CPE surface (B) the synthesis of U-IIP. Reprinted with permission from ref. [105], copyright 2020, Wang et al.

In a recent study, Zhong et al. [106] used a simple method of preparing the U-IIPs by using hydrothermal crosslinking of chitosan in the presence of uranyl ion as a template. The adsorption performance and other details of the materials are provided in Table 1.

Table 1. Uranyl ion-imprinted polymer materials, performance, and characterization.

Substrate	Components	Crosslinker	Method	Adsorption Capacity	pH	Characterization	Ref.
Si-C=C	MAA	EGDMA	FRP	35.92 mg/g	5	FTIR, SEM, EDX.	[60]
-	Na-Alg, Acroylinitrile	Glutarldehyde	Condensation	155 mg/g	5	FTIR, SEM, XRD, XPS	[72]
CMC	Acrylonitrile, SAL, thiourea	Formaldehyde	FRP	180 mg/g	5	FTIR, TGA, SEM	[79]
Fe_3O_4	MAA, SALO, 4-VP, Oleic acid	EGDMA	FRP	1.01 mg/g	4	FT-IR, Raman, SEM	[90]
Fe_3O_4	APS and TEOS	-	Sol-gel	25.8 µmol/g	4	FTIR, XRD, SEM	[92]
Fe_3O_4-SiO_2	HEMAA, VI	-	FRP	146.4 mg/g	5	FTIR, SEM, EDX.	[96]
-	(pyr_2en)DMSO 4-VP	Styrene	FRP	-	7	UV-VIS, IR, XRD	[99]
HQ-APTMS-SI	4-VP, HEMA	EGDMA	FRP	97.1 µmol/g	6	FTIR, TEM, SEM	[100]
-	Chitosan and PVA	EGDMA	Condensation	132 mg/g	5–6	FTIR	[101]
Fe_3O_4	Chitosan	Glutaraldehyde	Crosslinking	187.3 mmol/g	5	FTIR, XRD, SEM	[102]
-	DPTES, P123, TEOS	-	Condensation	80 mg/g	5.9	FTIR, SEM, TEM, ^{31}P NMR, TGA	[103]
HPC	-	-	Carbonization	503.64 mg/g	8	SEM, XRD, XPS, FTIR	[104]
GR/CPE	IPTP, APTES, TEOS	-	Sol-gel	-	5	FTIR, EDS, SEM	[105]
-	Chitosan	-	Hydrothermal	408.2 mg/g	7	FTIR, EDS, SEM	[106]
-	Methacrylic acid and triethylamine	EGDMA	FRP	23.9 mg/g		FTIR, TGA	[107]
γ-MPS-Fe_3O_4	SALO, 4-VP, MAA	EGDMA	FRP	-	4.3	FTIR, SEM	[108]
-	Salicyaldehyde, p-aminostyrene,	DVB	FRP	147.8 mg/g	5	^{1}H and ^{13}C NMR, FT-IR, SEM	[109]
Carbon powder	AQ, ICTMS	-	Sol-gel	-	5	SEM	[110]

4.2. Thorium

Being the first true actinide, thorium still has an empty 5f orbital, and therefore Th(IV) is the most stable and plentiful oxidation state [111]. The IIPs are an excellent choice for Th^{4+} removal due to their selectivity and retention capacity. Lin et al. [112] prepared Th^{4+}-IIP using a new pyrazole derivative—1-phenyl-3-methylthio-4-cyano-5-acrylicacidcarbamoylpyrazole—as a complexing monomer and by using carboxylic acid-functionalized silica modified with maleic anhydride in the presence Th^{4+} as a template. In another work of Lin et al. [78], methacrylic acid as a complexing agent and modified carboxylic acid-functionalized silica were used for Th-IIP preparation. Similarly, a modified silica with acryloyl chloride and dibenzoylmethane used as metal chelating agent was presented by Ji et al. [80]. The magnetic Th-IIPs prepared by He et al. [113] apply a novel complex—N,N′-bis(3-allyl salicylidene) *o*-phenylenediamine (BASPDA)—on the surface of Fe_3O_4-SiO_2. Magnetic chitosan crosslinked with epichlorohydrin (ECH)-based Th-IIPs were prepared by Huang et al. [114] where the adsorption performance was investigated. Othman et al. [115] reported radiation-induced copolymerization of 2-hydroxyethyl methacrylic phosphoric acid diester (2-HMPAD) and 2-hydroxyethyl methacrylic phosphoric acid monoester (2-HMPAA)–thorium ion complex using as crosslinker DVB or EGDMA where the base represents a non-woven fabric made of polypropylene/polyethylene. The adsorption performance of IIPs mentioned above is presented in Table 2.

Table 2. Thorium ion-imprinted polymer materials, performance, and characterization.

Substrate	Components	Crosslinker	Method	Adsorption Capacity	pH	Characterization	Ref.
SiO_2-modified MA	MAA	EGDMA	FRP	7.3 mg/g	3	FTIR, UV-VIS	[78]
SiO_2-NH_2	DBM, β-CD	EGDMA	FRP	30.8 mg/g	3.5	FT-IR, XPS, SEM	[80]
-	PMTCAAP	EGDMA	FRP	64.8 mg/g	3.5	UV-VIS, FTIR, ^{1}H NMR	[112]
Vinyl functionalized Fe_3O_4 SiO_2-NH_2	BASPDA	EGDMA	FRP	42.54 mg/g	4.5	FTIR, XRD	[113]
Fe_3O_4	Chitosan	ECH	Condensation	147.7 mg/g	4	FTIR, EDX	[114]
-	2-HMPAD, 2-HMPAA	EGDMADVB	FRP	-	3.5	FTIR, SEM, XPS.	[115]

4.3. Cesium

To capture the cesium from the environment, different materials based on carbon, titanate, tungstate, vanadate, hydroxyapatite, metal oxides were used [108,109,111,112,116,117]. IIPs based on these sorption materials were investigated in various studies. Zhang et al. [118] prepared sodium trititanate whiskers (STWs) supported by a chitosan ion-imprinted polymer for the selective capture of the Cs^+ from aqueous solutions (Figure 6).

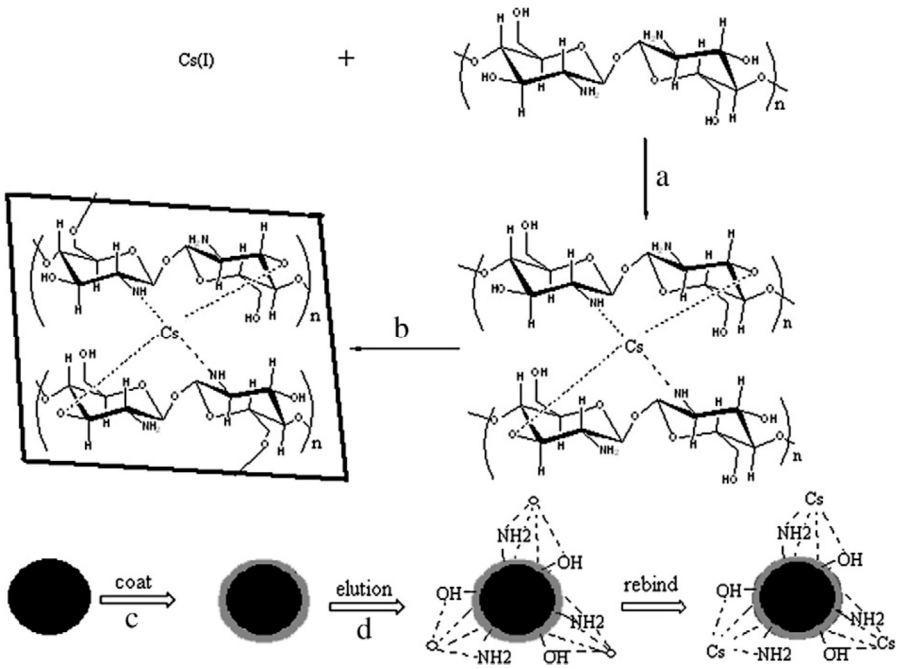

Figure 6. Schematic presentation of the preparation of chitosan Cs^+ imprinted polymer-coated whiskers. Reprinted with permission from ref. [115], copyright 2020, Othman et al.

Shamsipur et al. [119] prepared Cs-dibenzo-24-crown-8 (DB24C8) chelate imprinted nanoparticles by a precipitation polymerization method. Iwasaki et al. [120] prepared polyacrylonitrile (PAN)-based Cs^+-IIP for Cs adsorption from nuclear waste. Meng et al. [91] prepared two novel Cs^+-IIPs by a surface imprinting technique supported by a SBA-15 mesoporous silica matrix. The polymerization was carried out using two different RAFT (Figure 7). Other important properties and details of the aforementioned IIPs are presented in Table 3.

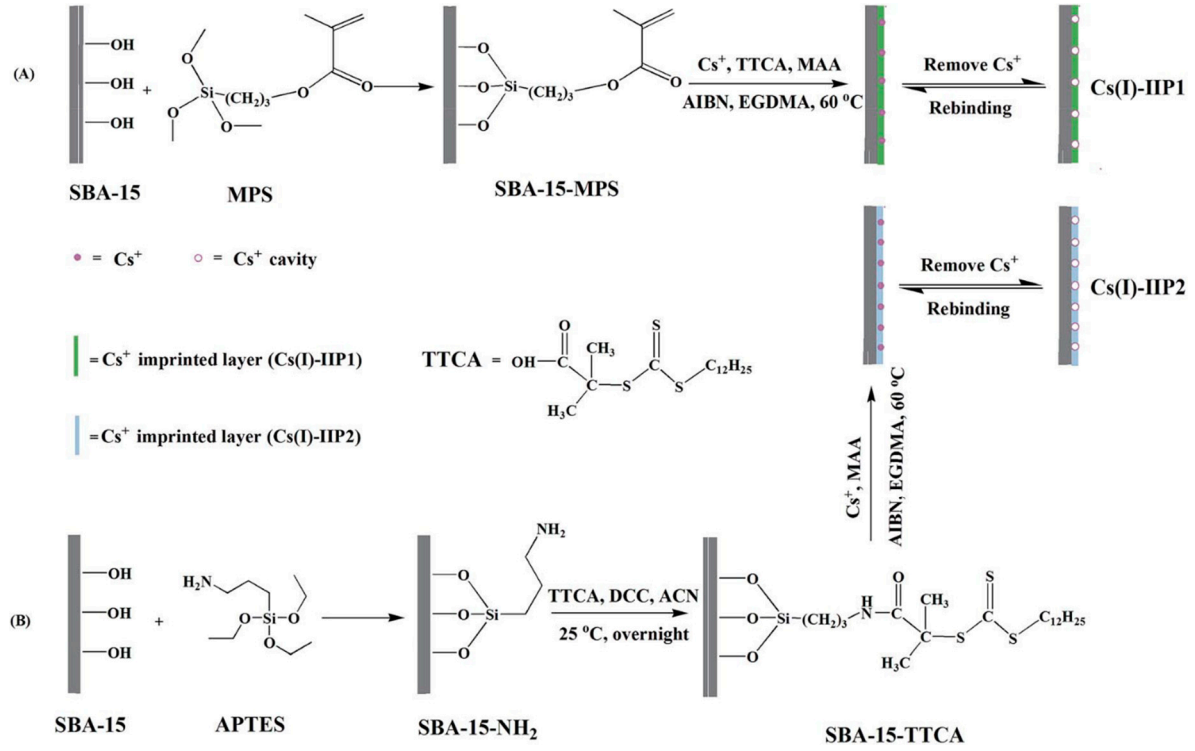

Figure 7. Schematic presentation of two different Cs^+-IIP, via RAFT polymerization techniques: (A) preparation of Cs(I)-IIP1 (B) preparation of Cs(I)-IIP2. Reprinted with permission from ref. [91], copyright 2015, Meng et al.

Table 3. Cesium ion-imprinted polymer materials, performance, and characterization.

Substrate	Components	Crosslinker	Method	Adsorption Capacity	pH	Characterization	Ref.
SBA-15	MAA	EGDMA	RAFT	54.54 mg/g	6	FTIR, SEM, EDS	[91]
STW	Chitosan	KH-560	Condensation	32.88 mg/g	6	FTIR, XRD	[118]
-	DB24C8, MAA	EGDMA	FRP	-	9	SEM	[119]
-	PAN	-	Spin casting	-	-	SPR	[120]

4.4. Strontium

^{90}Sr is produced in the nuclear fission process of ^{235}U and from nuclear weapons testing. In the environment it occurs in the 2+ oxidation state [121]. For Sr^{2+} removal, Liu et al. [122] used PTW and chitosan for IIP preparation. The PTW has mechanical and chemical stability and excellent wear-resistance properties. The chitosan was grafted on the surface of the PTW using a GPTMS silane coupling agent. Li et al. [11] have prepared strontium ion-imprinted hybrid gels from bis(trimethoxysilylpropyl) amine (TSPA) for the removal of Sr^{2+} and Ca^{2+} ions using dicyclohexano-18-crown-6, methacrylic acid (MAA), EGDMA removal. For the determination of Sr^{2+} in urine samples, Baharin et al. [123] prepared Sr^{2+}-IIP by using dicyclohexano-18-crown-6 (D18C6), MAA, and EGDMA as the crosslinker. Palygorskite offers promising properties such as high surface area, mechanical and chemical stability. Pan et al. [124] prepared palygorskite and chitosan-based Sr-IIP hollow spherical beads. Microorganisms such as yeast formed the support for the preparation Sr-IIP used by Song et al. [94]. In this preparation, a composite silica/yeast was generated by the Stober method. The prepared composite was crosslinked with chitosan with KH-560. Liu et al. [125] developed a thermally responsive IIP based on SBA-15 mesoporous silica loaded with magnetic polyethyleneimine. The free-radical polymerization of vinyl monomers methacryloxypropyltrimethoxysilane (MEMO), *N*-isopropylacrylamide (NIPAM) and *N,N*-methylenebisacrylamide (MBAA) were used, which were polymerized onto the surface of the prepared silica.

Research on graphene and graphene oxide-based materials is currently at the forefront due to graphene's properties such as 2D dimensional layered structure, mechanical, thermal, and chemical properties. Liu et al. [82] prepared a novel hydrophilic graphene oxide IIP using methacrylic acid in the surface imprinting method for Sr^{2+}, which is depicted in Figure 8.

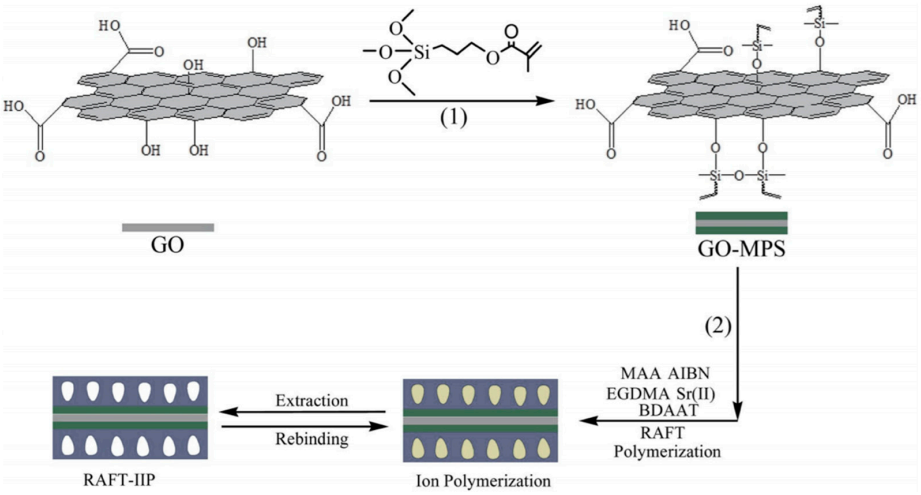

Figure 8. Schematic presentation of graphene oxide-based Sr-IIP. Reprinted with permission from [82], copyright 2015, Liu et al.

Dithiocarbomate ($-S_2CNR_2$) can form strong metal-carbon bonds. This aspect favors dithiocarbomate-grafted chitosan Sr-IIP preparation. To achieve dithiocarbomate functionalization on chitosan beads, Liu et al. [93] applied the four steps depicted in Figure 9. The important data of Sr-IIPs are presented in Table 4.

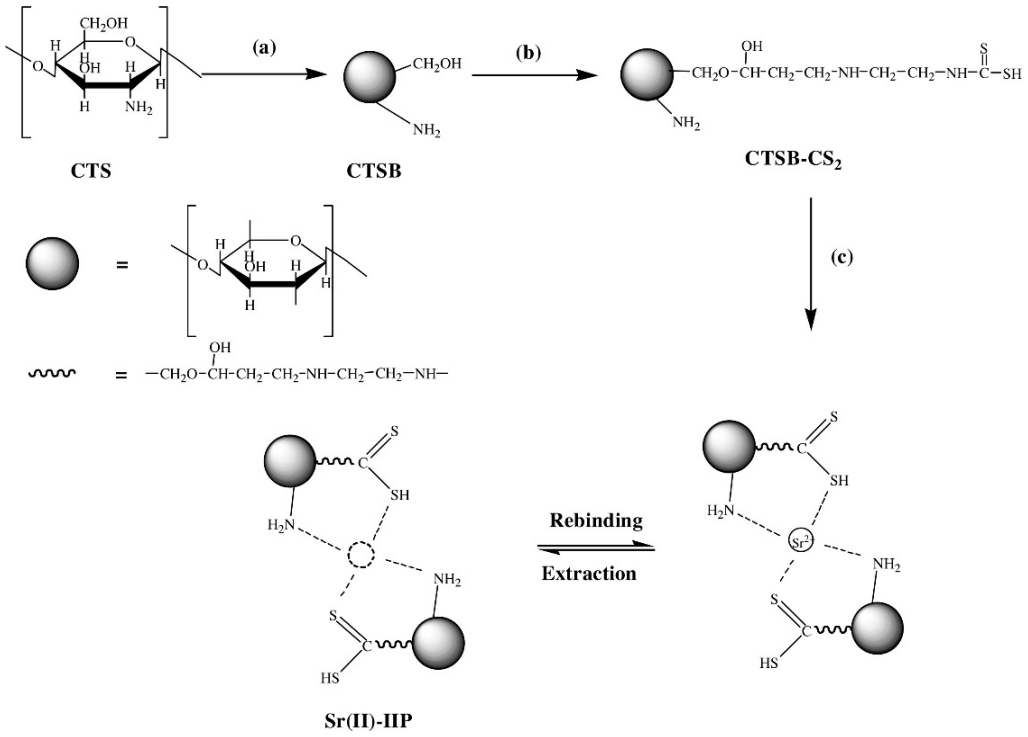

Figure 9. Schematic presentation of the dithiocarbomate functionalized chitosan Sr IIP preparation. Reprinted with permission from ref. [93], copyright 2015, Liu et al.

Table 4. Strontium ion-imprinted polymer materials, performance, and characterization.

Substrate	Components	Crosslinker	Method	Adsorption Capacity	pH	Characterization	Ref.
-	TSPA	-	Sol-gel	-	7	-	[11]
Graphite	MAA, MPS	EGDMA	RAFT	145.8 mg/g	6	FTIR, UV-VIS, SEM, TEM, XRD, AFM	[82]
-	Chitosan, CS_2	Glutaraldehyde	Condensation	86.66 mg/g	6	FTIR, XPS, ICP, SEM, FAAS	[93]
Yeast	TEOS, chitosan	KH-560	Condensation	60.6 mg/g	6	FTIR, SEM, SEM, TEM	[94]
-	D18C6, MAA	EGDMA	FRP	-	6.3	FTIR, LSA	[123]
Palygorskite	Chitosan	KH-560	Condensation	45 mg/g	4	FTIR, SEM	[124]
Fe_3O_4-SBA-15	MPS, MAA, NIPAM	BIS	FRP	89 mg/g	7	FTIR, XRD, TGA, SEM	[125]
SBA-15	MAA, TTCA	EGDMA	FRP	22.12 mg/g	6	FTIR, SEM, TEM	[126]

4.5. Cerium

Cerium is one of the most abundant rare earth metals, and the cerium isotopes with the longest half-life are ^{144}Ce, ^{139}Ce, and ^{141}Ce, produced by uranium fission [127]. Pan et al. [128] prepared chitosan-based Ce^{3+}-IIP crosslinked with the γ-3-glycidoxypropyltrimethoxysilane (KH-560) for Ce sorption. Zhang et al. [129] utilized PTW as a base and used a surface imprinting process for PTW and chitosan Ce^{3+} ion-imprinted polymer preparation. Chen et al. [81] developed a carbon paste electrode modified with ion-imprinted polymer for the trace detection of Ce^{3+}. Prasad et al. [130] prepared double IIP sensors for the detection of Ce^{4+} and Gd^{3+} ions. The polymer was prepared using free radical polymerization. The magnetic nanoparticle -COCl was spin-coated on the surface of the screen-printed carbon paste electrode after which it was polymerized with multiwalled carbon nanotubes (MWCNT) in the presence of Ce^{4+} and Gd^{3+} template ions (Figure 10).

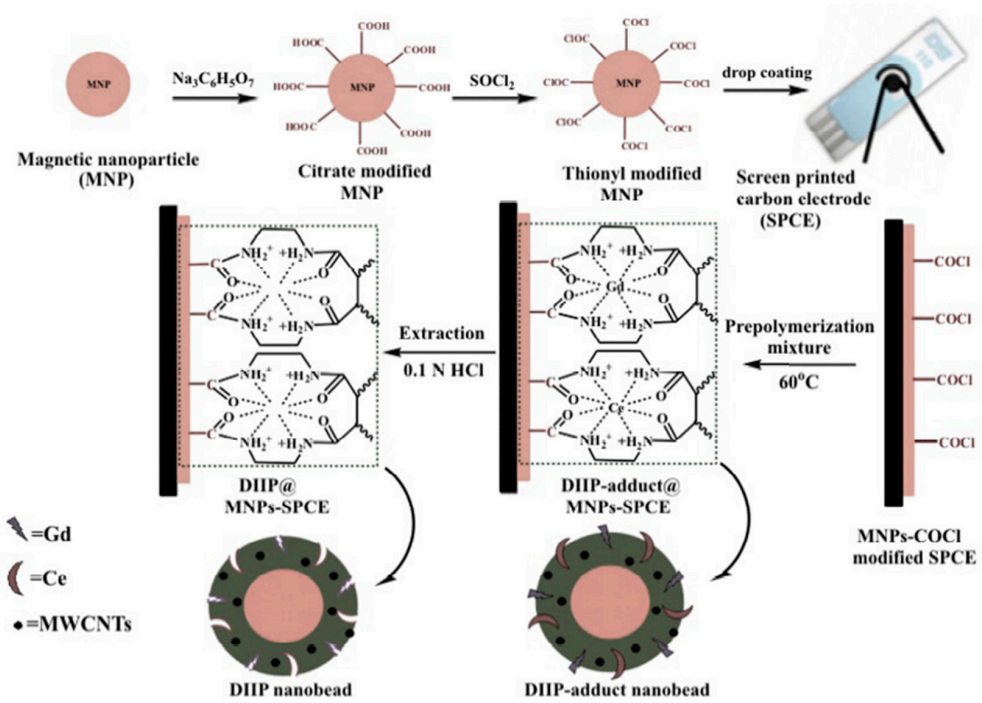

Figure 10. Schematic presentation for the development of the Ce^{4+} and Gd^{3+} ion-imprinted polymer-coated sensors. Reprinted with permission from ref. [130], copyright 2015, Prasad et al.

In another study, Alizadeh et al. [131] prepared a modified carbon electrode with Ce^{3+}-IIP ion-imprinted polymer. The monomer used in this 4-vinylpyridine and MAA preparation was polymerized in the presence of $Ce(NO_3)_3$ as a template. Kecili et al. [132] synthesized Ce^{3+}-IPP cryogel by using 2-hydroxyethyl methacrylate (HEMA) and *N*,*N*-

methylenebisacrylamide (MBAAm), cryopolymerization, resulting in poly(HEMA-co-$(MAAP)_2Ce(H_2O)_2$. Liu et al. prepared SBA-15-supported chitosan crosslinked with KH-560 imprinted polymer for Ce^{3+} removal [128]. The adsorption performance and other physical and chemical properties of the abovementioned IIPs are mentioned in Table 5.

Table 5. Cerium ion-imprinted polymer materials, performance, and characterization.

Substrate	Components	Crosslinker	Method	Adsorption Capacity	pH	Characterization	Ref.
Graphite	APA	EGDMA	FRP	-	-	-	[81]
PTW	Chitosan	KH-560	Condensation	-	6	FTIR, XRD,	[129]
MNPs, SPCE	-	EGDMA	FRP	-	-	SEM	[130]
MWCN	MAA, VP	DVB	FRP	-	-	SEM	[131]
-	HEMA, MBAAm	-	Cryolpoymerisation	-	6–7	FTIR, SEM, EDX, UV	[132]
SBA-15	Chitosan	KH-560	Condensation	-	5	FTIR, XRD, SEM	[133]

4.6. Technetium

Technetium has several different oxidation states in Nature. The oxidation state 7+ is generally the most common in the environment. The pertechnetate ion (TcO_4^-) is generated in large amounts from nuclear waste, and its mitigation strategy is a key concern [134]. In recent literature, Shu et al. [96] prepared a perrhenate ion-based imprinted polymer by using the surface imprinting method. The perrhenate ion is the structural surrogate and carrier of TcO_4^- depicted in Figure 11. The preparation was carried out by applying a surface imprinted strategy, the 4-vinylbenzyl chloride and *N*-vinylimidazole(VI) were polymerized on the surface of vinylated Fe_3O_4-SiO_2. The adsorption capacity was studied using the Langmuir model. The adsorption capacity was found to be equal to 62.8 mg/g at pH = 6 and a temperature of 298.15 K.

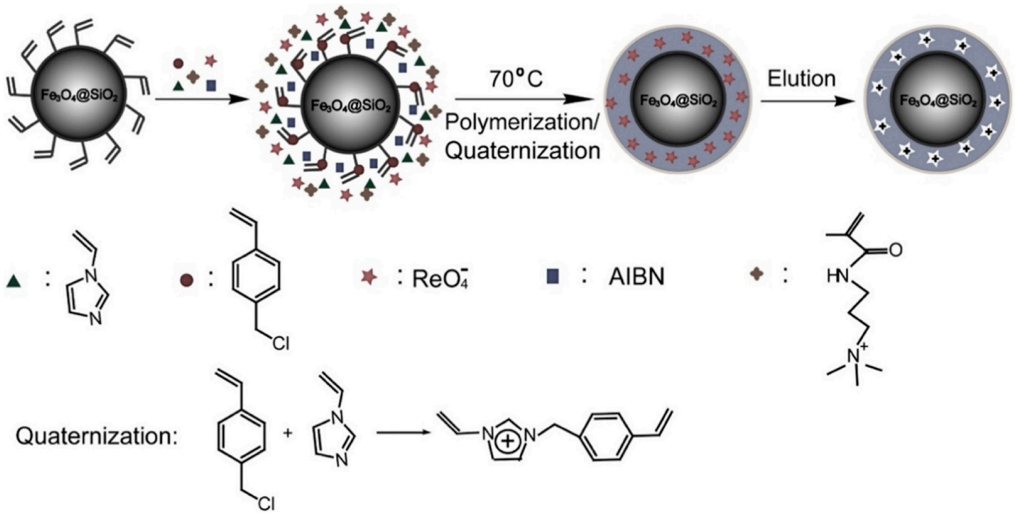

Figure 11. Schematic presentation of pertechnetate IIP preparation. Reprinted with permission from ref. [96], copyright 2015, Shu et al.

4.7. Lanthanum

Among rare earth metals, lanthanum is the most abducent one; interest in it has expanded because of its unique physical and chemical properties. Many conventional methods for removing radionuclides and lanthanides from aqueous solutions were already presented [135]. Ion-imprinted materials explicitly and specifically target a metal ion based on their charge and shape. In a recent study, Wang et al. [136] used straw as a base for the preparation of a La^{3+} ion-imprinted polymer using the surface-initiated atom transfer radical polymerization (ATRP) method which is helpful for making homogenous polymer coatings on various surfaces using monomers such as *N*,*N*,*N*′,*N*′,*N*″-

pentamethyldiethylenetriamine (PMDETA), *N*,*N*-dimethylaminoethyl methacrylate (DMAEMA), polymerized by thermal radical polymerization and crosslinked using EGDMA. In another study, Mustapa et al. [137] prepared La- and Ce-based IIPs using a Schiff base ligand ((ethyl 4-(2,4-dihydroxybenzylideneamino) benzoate), or an azobenzene ligand ((4-(2,4-dihydroxyphenylazo) acetophenone) and La^{3+} adsorption was studied in the presence of (Pr^{3+}, Nd^{3+}, and Pm^{3+})—the elements have approximately the same nuclear radius. The prepared IIPs showed promising results for La removal. Besharati-Seidani et al. [138] developed the La^{3+} ion-imprinted nanoparticles (NPs) using the La^{3+}-chelating ligand 2,2′:6′,2″-terpyridine (terpy). The adsorption and desorption cycle for this material was completed within 2 to 30 min. Other properties of these IIPs are summarized in Table 6.

Table 6. Lanthanum ion-imprinted polymer materials, performance, and characterization.

Substrate	Components	Crosslinker	Method	Adsorption Capacity	pH	Characterization	Ref.
Straw	PMDETA, DMAEMA	EGDMA	ATRP	125 mg/g	6	XPS, SEM, FTIR	[136]
-	Schiff base, and Azobenzene	EGDMA	FRP	25 mg/g 24 mg/g	7	FTIR, FE-SEM, UV-VIS	[137]
	Terpy	EGDMA	FRP	133.8 mg/g	3.5	FTIR, UV, SEM.	[138]

4.8. Chromium

Recently, for effective binding of Cr ions, a new type of IIPs was developed. Trzonkowska et al. [139] prepared Cr-IIP by using 1,10-phenanthroline ligand. The ligand was polymerized with MAA/ST and crosslinked using EGDMA. The prepared IIPST-AIBN is found to have good adsorption efficiency, rapid adsorption kinetics and desorption, and resistance to competitive ions. In another study, Liang et al. [140] developed surface imprinted Cr-IIP using Fe_3O_4-SiO_2 as a support medium. The polymerization has been done using 4-VP and HEMA or EGDMA as a crosslinker. A similar type of study was carried out by Zhou et al. [141] where Fe_3O_4-SiO_2 was modified with MPS and after surface imprinting polymerization was accomplished by using 4-VP. Kumar et al. [142] used a three-step preparation of chromium-based magnetic IIPs. The first one was the preparation of silica modified Fe_3O_4-NPs, in the second step it was modified with amine (Fe_3O_4-SiO_2-NH_2). Finally, in the third step, the NPs were coated with polymer using 4-VP and MAA, and EGDMA as the crosslinker. Table 7 presents the adsorption performance and other characteristics of Cr-IIPs.

Table 7. Chromium ion-imprinted polymer materials, performance, and characterization.

Substrate	Components	Crosslinker	Method	Adsorption Capacity	pH	Characterization	Ref.
-	1,10-phenanthroline complex, styrene, MAA	EGDMA	Bulk polymerization	-	4.5	FTIR, SEM	[139]
Fe_3O_4-SiO_2	4-VP, HEMA	EGDMA	FRP	311.95 mg/g	2	FTIR, SEM-EDS, XRD, TGA	[140]
Fe_3O_4-SiO_2	4-VP	EGDMA	FRP	131.40 mg/g	2	FTIR, XPS, TEM, TGA	[141]
Fe_3O_4-SiO_2-NH_2	4-VP, MAA	EGDMA	FRP	169.49 mg/g	2	FTIT, SEM-EDS	[142]

4.9. Nickel

For the selective detection and removal of Ni^{2+}, a novel ion-imprinted polymer was developed. Zhou et al. [143] prepared a Ni^{2+}-imprinted polymer by bulk polymerization. Ligands such as diphenylcarbazide (DPC) and *N*,*N*-azobisisobutyronitrile (AIBN) were used for Ni^{2+} adsorption. The study of Ni^{2+} removal from aqueous solutions using surface-modified molecularly imprinted ferrite nanomaterials as adsorbent was carried out by Ahmad et al. [144]. They used ferrous and ferric salts for the development of molecularly imprinted ferrite in a primary medium. A silica coating was applied in the Stober process and the sol-gel method using TEOS and TNT. In another study concerned with the selective Ni removal and proper complexation with Ni ions, an ion-imprinted material was prepared with diacetylmonoxine-modified chitosan. To maintain the structural rigidity of

the polymer, glyoxal was used as a crosslinker [145]. Lenoble et al. [146] prepared a Ni^{2+} imprinted polymer using *N*-(4-vinylbenzyl)-2-(aminomethyl)pyridine (Vbamp) ligand to form a complex between Ni^{2+} and the complex crosslinked with EGDMA in a 1:3 ratio. The prepared material showed excellent retention capacity over other competitive ions. The properties of the abovementioned Ni-IIPs are presented in Table 8.

Table 8. Nickel ion-imprinted polymer materials, performance, and characterization.

Substrate	Components	Crosslinker	Method	Adsorption Capacity	pH	Characterization	Ref.
	DPC, MAA	EGDMA	FRP	86.3 mg/g	7	FTIR, SEM, XRD, EDX	[143]
Fe_3O_4-SiO_2	TNT, TEOS	-	Sol-gel	2.64 mg/g	7.6	FTIR, SEM, EDX, XRD	[144]
diacetylmonoxine modified chitosan	-	glyoxal	Condensation	135 mg/g	5	FTIR, XRD, ^{1}H NMR, ^{13}C NMR, SEM, EDX	[145]
-	Vbamp	EGDMA	FRP		4–7	FTIR, UV-VIS, SEM	[146]

4.10. Cobalt

Cobalt is one of the heavy metals that can cause several adverse health effects on humans, e.g., pneumonia, goiter, and gastrological diseases [147,148]. Cobalt has several isotopes, ^{60}Co, ^{58}Co, ^{57}Co that are highly radioactive gamma emitters. Exposure to these isotopes causes hair loss, skin burns, anemia, and cancer [149]. Recently, IIPs have gained significant interest in removing Co^{2+} ions due to their selectivity and recognition ability. The use of inorganic materials (such as palygorskite, titanate whiskers, SBA-15) grafted on chitosan or polyethyleneimine, which have been crosslinked with epoxy functionalized organic or silane coupling agents, for the Co-IIPs preparation, are explored in various studies [150–153]. Figure 12 presents a method used for the synthesis of IIPs from chitosan.

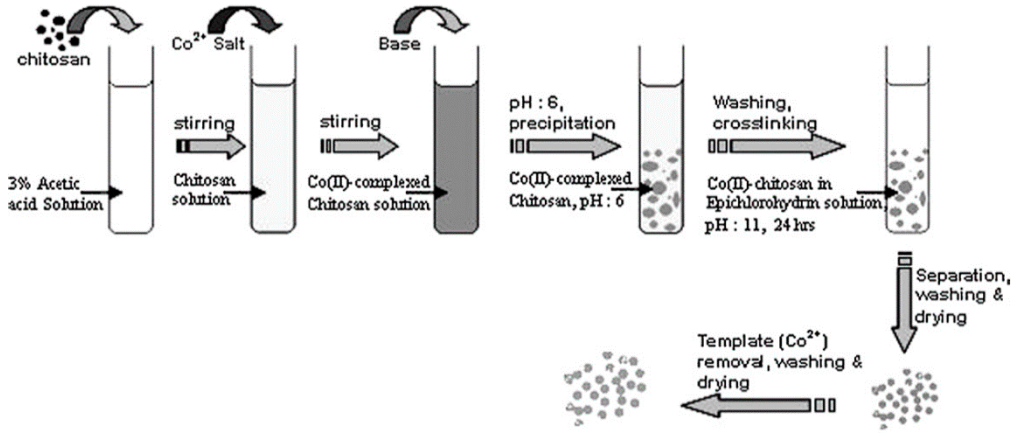

Figure 12. Schematic presentation of Co-IIP prepared from crosslinked chitosan. Reprinted with permission from ref. [154], copyright 2012, Mishad et al.

Nishad et al. [154] prepared Co-IIP from chitosan crosslinked using epichlorohydrin. Bhaskarpillai et al. [155] reported the stability of the complex between cobalt and vinylbenzyliminodiacetic acid (VbIDA) and successfully prepared its Co-IIP. Liu et al. [156] prepared a cysteine -rafted chitosan-based imprinted polymer for Co^{2+} and Mn^{2+} ions. Kang et al. [95] prepared a novel Co-IIP using hydrophilic monomer 1-vinylimdazole (1-VI) surface imprinted on Fe_3O_4-SiO_2 magnetite nanoparticles. The method is depicted in Figure 13.

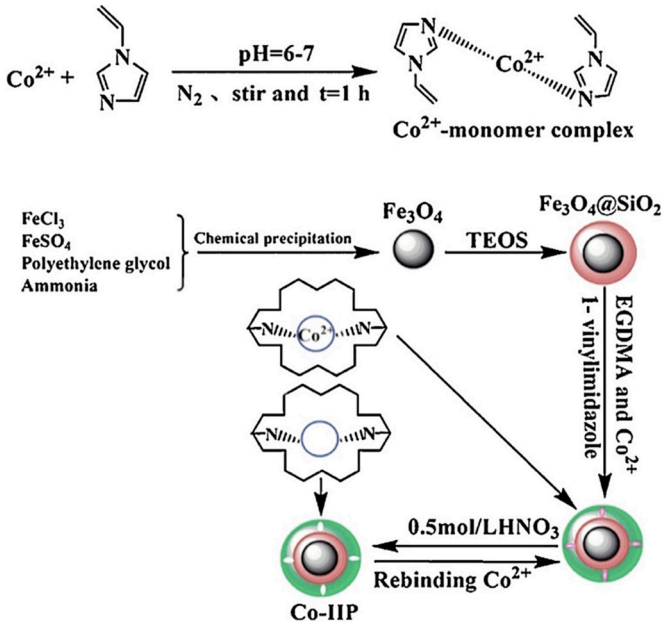

Figure 13. Schematic presentation of the route of preparation of Co-IIP. Reprinted with permission from ref. [95], copyright 2016, Kang et al.

The use of activated carbon modified with -COOH groups as a crosslinker with hydrazine hydrate for the preparation of Co-IIP was developed by Turan et al. [157]. Metal-organic frameworks (MOF) have interesting properties such as high porosity, a wide range of structural possibilities and tunable porous sizes. Yuan et al. prepared a Co-IIP from MOF based on 2-aminoterephthalic acid (NH_2-H_2BDC) modified with glycylglycine [158]. Torkashvand et al. developed a Co-IIP as a voltammetric sensors, aiming for Co^{2+} tracer determination, using Co^{2+}-8-hydroxyquinoline linked to cast magnetic nanoparticles at a glass carbon electrode surface. The procedure is illustrated in Figure 14 [159].

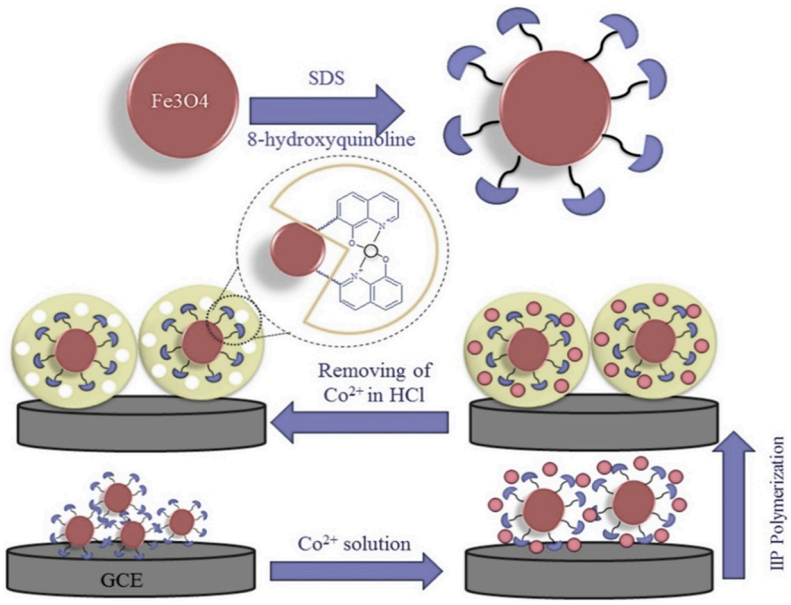

Figure 14. The development of the Co-IIP based voltammetric sensors. Reprinted with permission from ref. [159], copyright 2017, Torkashvand et al.

In another study, Sebastian et al. [160] developed Co-IIP sensors from multi-walled carbon tubes modified with vinyl groups and crosslinked with N,N′-methylenebis(acrylamide)

(NNMBA). Yusof et al. [161] developed dipicolinic acid (DPA)-based Co-IIP by free radical polymerization. Bovine serum albumin (BSA) can go through various conformational and structural changes after reacting with different metal ions via its amino acid residues [162]. Li et al. [163] prepared a Co^{2+}-BSA-CO chelated complex. It was introduced as template in a nanocomposite designed from a multi-walled carbon nanotube, Cu nanoparticles and carbon quantum dots-based Co-IIP sensors. Lee et al. [164] used magnetic silica to prepare a Co-IIP with the concern of its main use for nuclear powerplant decontamination. Adibmehr et al. [165] developed novel cobalt ion-imprinted polymer using mesoporous silica SBA-15 modified with (3-chloropropyl)triethoxysilane, and EGDMA as a crosslinker. Biswas et al. [166] prepared curcumin-based ion-imprinted polymer for the selective removal of Co, Cd and Pb ions. The other important parameters of CO-IIPs are presented in Table 9.

Table 9. Cobalt ion-imprinted polymer materials, performance, and characterization.

Substrate	Components	Crosslinker	Method	Adsorption Capacity	pH	Characterization	Ref.
Fe_3O_4-SiO_2	1-VI	EGDMA	FRP	23.09 mg/g	6–7	FTIR, SEM	[95]
Palygorskite	Chitosan	Condensation	31.5 mg/g		4	FTIR, SEM	[151]
SBA-15	PEI	ECH	Condensation	39.36 mg/g	7	FTIR, SEM, XRD	[152]
STW	Chitosan	KH-560	Condensation	33.7 mg/g	5	FTIR, SEM	[153]
-	Chitosan	ECH	Condensation	75 µmol/g	4.8	-	[154]
-	Cu(VbIDA)	EDGMA	FRP	205 µmol/g	5	EPR	[155]
-	Cytesine, chitosan	ECH	Condensation	-	5.58	FTIR, SEM	[156]
AC-COOH	Hydrazine hydrate	-	condensation	833.7 mg/g	7	FTIR, SEM	[157]
MOF	NH_2-H_2BDC, $ZrCl_4$, glycine	-	-	175 mg/g	8.4	FTIR, SEM, XRD	[158]
8-HQ modified Fe_3O_4	AAM,	NNMBA	FRP	-	9	FTIR, SEM	[159]
Vinyl functionalized MWCNT	Acrylic acid	NNMBA	FRP	-	6	FTIR, SEM, EDAX, TGA	[160]
-	MAA,4-VP	EGDMA	FRP	106 mg/g	6	FTIR, SEM	[161]
MWCNT	BSA, Carbon dots, PVP	-	-	-	7.8	XPS, SEM	[163]
Fe_3O_4-SBA-15	TEOS, P123	-	Sol-gel	74 mg/g	8	FTIR, SEM, TGA	[165]
-	Curcumin, acrylic acid	EGDMA	FRP	105 mg/g	6	UV-VIS, FTIR, SEM	[166]

5. Conclusions

In this review article, ion-imprinted polymers for the adsorption of 10 important radionuclides—U, Th, Cs, Sr, Ce, Tc, La, Cr, Ni, Co—which are found in the nuclear fuel cycle, are presented. These radionuclides were chosen for this study due to their commercial interest and environmental concerns. Recent updates in the field of ion-imprinted polymers for the radionuclide separation discussed with preparation methods, properties, adsorption capacities, and characterization methods used for its determination were discussed here. In recent years, research interest has been focused on the development of ion-imprinted polymers for radionuclide separation due to their properties such as selectivity and recognition ability for targeted ions. Despite the number of studies in this area, more research should be done on TcO_4^- and Ce^{3+}. Ion-imprinted polymers are based on organic substances that have a huge variability and complex formation abilities with metallic ions whereas inorganic-based materials show excellent thermal and environmental stress-related stability. The combination of both organic- and inorganic-based ion-imprinted polymers allow good preservation of their properties. On the other hand, there are some issues related to ion-imprinted polymers, e.g., regarding their lower reusability and large-scale production. The understanding of the chelating mechanism is important for future research aimed at improving the binding performance of ion-imprinted polymers. Indeed, concerning ligands and functional monomers, this can be achieved by computational methods. Other ways to improve the selective adsorption are by utilizing novel selection methods such as surface imprinting, stimuli-responsive imprinting, and dual/multiple component imprinting. New preparation techniques should be explored for better selectivity, cost reduction, and large-scale production of ion-imprinted polymers.

Author Contributions: Conceptualization, M.G. and V.V.K.; resources, V.V.K.; M.G. and E.V.; data curation, V.V.K.; writing—original draft preparation, V.V.K.; M.G.; E.V.; J.Š.; writing—review and editing, M.G.; M.D.; E.V. and J.Š.; visualization, V.V.K.; supervision, M.G.; funding acquisition, M.G.; E.V. and J.Š. All authors have read and agreed to the published version of the manuscript.

Funding: This research was funded by APVV agency, Project No. APVV-18-0534. This work was also performed under the auspices of Ministry of Education Youth and Sports; Project Nr. CZ.02.1.01/0.0/0.0/16_019/0000728: "RAMSES—Ultra-trace isotope research in social and environmental studies using accelerator mass spectrometry" is funded by MEYS and European Union—European Structural and Investment Funds, Operational Programme Research, Development and Education.

Institutional Review Board Statement: Not applicable.

Informed Consent Statement: Not applicable.

Data Availability Statement: Data is contained within the article.

Conflicts of Interest: The authors declare no conflict of interest. The funders had no role in the design of the study; in the collection, analyses, or interpretation of data; in the writing of the manuscript, or in the decision to publish the results.

Abbreviations

1-VI	1-Vinylimdazole
2-HMPAAD	2-Hydroxyethyl Methacrylic Phosphoric Acid Diester
2-HMPAAM	2-hydroxyethyl methacrylic phosphoric acid monoester
4-VBC	4-Vinylbenzyl Chloride
4-VP	4-Vinyl Pyridine
4-VP	4-Vinylpyridine
8-HQ	8-Hydroxyquinoline
AAM	Acryl amide
ABDV	Azobisdimethylvaleronitrile
AIBN	Azobisisobutyronitrile
AIBN	N,N-Azobisisobutyronitrile
AFM	Atomic Force Microscopy
AP	Activation Products
APS	3-Aminotriethoxy Silane
APTS	(3-aminopropyl) triethoxysilane
ATRP	Atom Transfer Radical Polymerization
BASPDA	*N, N′*-Bis(3-Allyl Salicylidene) O-Phenylenediamine
BIS	N,N -Methylenebisacrylamide
BPO	Benzoylperoxide
BSA	Bovine Serum Albuminmetal
CMC	Carboxymethyl cellulose
CPE	Carbon paste electrode
CPMA	N-(O-Carboxyphenyl) Maleamic Acid
CTS	Chitosan
D-R	Dubinin-Radushkevitch
D18C6	Dicyclohexano-18-Crown-6
DB24C8	Dibenzo-24-Crown-8
DBM	Dibenzoylmethane
DCQ	5,7-Dichloroquinoline-8-Ol
DMAEMA	*N,N′*-Dimethylaminoethyl Methacrylate
DMSO	Dimethyl sulfoxide
DPA	Dipicolinic Acid
DPC	Diphenylcarbazide
DPTES	Diethylphosphatoethyltriethoxysilane
DVB	Divinylbenzene
FT-IR	Fourier transform infrared spectroscopy
ECH	Epichlorohydrin
EDX	Energy-dispersive X-ray spectroscopy

EGDE	Ethylene Glycol Diglycidyl Ether
EGDMA	Ethylene Glycol Dimethacrylate
EGDMA	Ethylene Glycol Dimethacrylate
FAAS	Flame atomic absorption spectrometry
FP	Fission Products
FRP	Free Radical Polymerization
GO	Graphene oxide
GPTMS	Glycidoxypropyltrimethoxysilane
GR	Graphene
HAQ	1-Hydroxy-2-(Prop-2′-Enyl)-9,10-Anthraquinone
HEMA	2-Hydroxyethyl Methacrylate
HLRW	High-Level Radioactive Waste
HQ-APTMS-SI	Quinoline-8-Ol Functionalized 3-Aminopropyltrimethoxysilane Modified Silica Nanoparticles
HPC	Hierarchical Porous Carbon Material
II-HPC	Ion-Imprinted Hierarchical Porous Carbon Material
IIPs	Ion-Imprinted Polymers
IPN	Interpenetration Networks
IPTP	Isophthalaldehyde-Tertrapyrrole
LSA	Liquid scintillation analysis
KH-560	γ-Glycidoxypropyltrimethoxysilane
MAA	Methacrylic Acid
MEMO	Methacryloxypropyltrimethoxysilane
MBBA	N,N Methylenebisacrylamide
MIPs	Molecularly Imprinting Polymers
MNP	Magnetic nanoparticle
MOF	Metal Organic Frameworks
MPS	3 -(Methacryloxy)Propyltrimethoxysilane
MWCNT	Multiwalled Carbon Nanotubes
NH_2-H_2BDC	2-Aminoterephthalic Acid
NIPAM	N-Isopropylacrylamide
NNMBA	*N*, *N*′ Methylene Bis Acrylamide
NPs	Nanoparticles
P123	Poly(Ethylene Glycol)-Block-Poly(Propylene Glycol)-Block-Poly-(Ethylene Glycol) Copolymer
PAN	Polyacrylonitrile
PEI	polyethyleneimine
PMDETA	*N*,*N*,*N*′,*N*′,*N*″-Pentamethyldiethylenetriamine
PMTCAACP	1-Phenyl-3-Methylthio-4-Cyano-5-Acrylicacidcarbamoyl-Pyrazole
PTW	Potassium Titanate Whiskers
PVA	Poly Vinyl Alcohol
PVP	Polyvinylpyrrolidone
RAFT	Reversible Addition Fragmentation Techniques (RAFT) Polymerization
RN	Radionuclides
RW	Radionuclide waste
SALO	Salicylaldoxime
SEM	Scanning Electron microscopy
SNF	Spend Nuclear Fuel
SPCE	Screen printed carbon electrode
SPR	Surface plasmon resonance
STW	Sodium Trititanate Whisker
STY	Styrene
TEOS	Tetraethyl Orthosilicate
TGA	Thermogravimetric analysis
Terpy	2,2′:6′,6′-Terpyridine
TNT	2,4,6-Trinitrotoluene
TRIM	Trimethylolpropane Trimethacrylate
TSPA	Bis(Trimethoxysilylpropyl) Amine
TTCA	S-1-dodecyl-S′-(α,α′-dimethyl-α″-acetic acid)trithiocarbonate

UV-VIS	Ultra violet visible spectroscopy
Vbamp	N-(4-Vinylbenzyl)-2-(Aminomethyl)Pyridine
Vbida	Vinylbenzyliminodiacetic Acid
VI	N-Vinylimidazole
γ-MPS	γ-methacryloxypropyltrimethoxysilane
β-CD	Beta-cyclodextrin
XPS	X-ray Photoelectron Spectroscopy
XRD	X-ray diffraction method

References

1. Keith, S.; Faroon, O.; Roney, N.; Scinicariello, F.; Wilbur, S.; Ingerman, L.; Llados, F.; Plewak, D.; Wohlers, D.; Diamond, G. *Toxicological Profile for Uranium*; Agency for Toxic Substances and Disease Registry: Atlanta, GA, USA, 2013.
2. Horne, G.P.; Zarzana, C.A.; Grimes, T.S.; Rae, C.; Ceder, J.; Mezyk, S.P.; Mincher, B.J.; Charbonnel, M.-C.; Guilbaud, P.; Saint-Louis, G. Effect of Chemical Environment on the Radiation Chemistry of N, N-Di-(2-Ethylhexyl) Butyramide (DEHBA) and Plutonium Retention. *Dalton Trans.* **2019**, *48*, 14450–14460. [CrossRef] [PubMed]
3. Augustine, S.; Gagnaire, B.; Adam-Guillermin, C.; Kooijman, S.A.L.M. Effects of Uranium on the Metabolism of Zebrafish, Danio Rerio. *Aquat. Toxicol.* **2012**, *118*, 9–26. [CrossRef]
4. Manaka, M.; Seki, Y.; Okuzawa, K.; Watanabe, Y. Uranium Sorption onto Natural Sediments within a Small Stream in Central Japan. *Limnology* **2008**, *9*, 173–183. [CrossRef]
5. Nordberg, G.F.; Fowler, B.A.; Nordberg, M.; Friberg, L. *Handbook on the Toxicology of Metals*; Academic Press: Amsterdam, The Netherlands, 2007; p. 1024.
6. Keith, S.; Wohlers, D.; Ingerman, L. *Toxicological Profile for Thorium*; Agency for Toxic Substances and Disease Registry: Atlanta, GA, USA, 2019.
7. Ding, H.; Zhang, X.; Yang, H.; Luo, X.; Lin, X. Highly Efficient Extraction of Thorium from Aqueous Solution by Fungal Mycelium-Based Microspheres Fabricated via Immobilization. *Chem. Eng. J.* **2019**, *368*, 37–50. [CrossRef]
8. Morsy, A.M.A. Performance of Magnetic Talc Titanium Oxide Composite for Thorium Ions Adsorption from Acidic Solution. *Environ. Technol. Innov.* **2017**, *8*, 399–410. [CrossRef]
9. Igarashi, Y.; Kogure, T.; Kurihara, Y.; Miura, H.; Okumura, T.; Satou, Y.; Takahashi, Y.; Yamaguchi, N. A Review of Cs-Bearing Microparticles in the Environment Emitted by the Fukushima Dai-Ichi Nuclear Power Plant Accident. *J. Environ. Radioact.* **2019**, *205*, 101–118. [CrossRef]
10. Ma, B.; Oh, S.; Shin, W.S.; Choi, S.-J. Removal of Co2+, Sr2+ and Cs+ from Aqueous Solution by Phosphate-Modified Montmorillonite (PMM). *Desalination* **2011**, *276*, 336–346. [CrossRef]
11. Li, Q.; Liu, H.; Liu, T.; Guo, M.; Qing, B.; Ye, X.; Wu, Z. Strontium and Calcium Ion Adsorption by Molecularly Imprinted Hybrid Gel. *Chem. Eng. J.* **2010**, *157*, 401–407. [CrossRef]
12. Guo, Y.; Zhang, S.; Lai, L.; Wang, G. Rare Earth Elements in Oolong Tea and Their Human Health Risks Associated with Drinking Tea. *J. Food Compos. Anal.* **2015**, *44*, 122–127. [CrossRef]
13. Li, Y.; Li, P.; Yu, H.; Bian, Y. Recent Advances (2010–2015) in Studies of Cerium Oxide Nanoparticles' Health Effects. *Environ. Toxicol. Pharmacol.* **2016**, *44*, 25–29. [CrossRef]
14. Colton, R. *The Chemistry of Rhenium and Technetium*; Interscience Publishers: London, UK; New York, NY, USA, 1965.
15. Iannicelli-Zubiani, E.M.; Stampino, P.G.; Cristiani, C.; Dotelli, G. Enhanced Lanthanum Adsorption by Amine Modified Activated Carbon. *Chem. Eng. J.* **2018**, *341*, 75–82. [CrossRef]
16. Boffetta, P.; Cardis, E.; Vainio, H.; Coleman, M.P.; Kogevinas, M.; Nordberg, G.; Parkin, D.M.; Partensky, C.; Shuker, D.; Tomatis, L. Cancer Risks Related to Electricity Production. *Eur. J. Cancer Clin. Oncol.* **1991**, *27*, 1504–1519. [CrossRef]
17. Fišera, O.; Šebesta, F. Determination of 59Ni in Radioactive Waste. *J. Radioanal. Nucl. Chem.* **2010**, *286*, 713–717. [CrossRef]
18. Mudipalli, A.; Zelikoff, J.T. *Essential and Non-Essential Metals*; Humana Press: Totowa, NJ, USA, 2017.
19. Taddei, M.H.T.; Macacini, J.F.; Vicente, R.; Marumo, J.T.; Sakata, S.K.; Terremoto, L.A.A. Determination of 63Ni and 59Ni in Spent Ion-Exchange Resin and Activated Charcoal from the IEA-R1 Nuclear Research Reactor. *Appl. Radiat. Isot.* **2013**, *77*, 50–55. [CrossRef]
20. Gault, N.; Sandre, C.; Poncy, J.-L.; Moulin, C.; Lefaix, J.-L.; Bresson, C. Cobalt Toxicity: Chemical and Radiological Combined Effects on HaCaT Keratinocyte Cell Line. *Toxicol. Vitr.* **2010**, *24*, 92–98. [CrossRef] [PubMed]
21. Mahar, A.; Wang, P.; Ali, A.; Awasthi, M.K.; Lahori, A.H.; Wang, Q.; Li, R.; Zhang, Z. Challenges and Opportunities in the Phytoremediation of Heavy Metals Contaminated Soils: A Review. *Ecotoxicol. Environ. Saf.* **2016**, *126*, 111–121. [CrossRef] [PubMed]
22. Kononova, O.N.; Bryuzgina, G.L.; Apchitaeva, O.V.; Kononov, Y.S. Ion Exchange Recovery of Chromium (VI) and Manganese (II) from Aqueous Solutions. *Arab. J. Chem.* **2019**, *12*, 2713–2720. [CrossRef]
23. Mollah, A.; Begum, A.; Rahman, M. Removal of Radionuclides from Low Level Radioactive Liquid Waste by Precipitation. *J. Radioanal. Nucl. Chem.* **1998**, *229*, 187–189. [CrossRef]
24. Khani, M.H.; Keshtkar, A.R.; Ghannadi, M.; Pahlavanzadeh, H. Equilibrium, Kinetic and Thermodynamic Study of the Biosorption of Uranium onto Cystoseria Indica Algae. *J. Hazard. Mater.* **2008**, *150*, 612–618. [CrossRef]

25. Montaña, M.; Camacho, A.; Serrano, I.; Devesa, R.; Matia, L.; Vallés, I. Removal of Radionuclides in Drinking Water by Membrane Treatment Using Ultrafiltration, Reverse Osmosis and Electrodialysis Reversal. *J. Environ. Radioact.* **2013**, *125*, 86–92. [CrossRef]
26. Abdi, S.; Nasiri, M.; Mesbahi, A.; Khani, M.H. Investigation of Uranium (VI) Adsorption by Polypyrrole. *J. Hazard. Mater.* **2017**, *332*, 132–139. [CrossRef]
27. Wang, J.; Zhuang, S. Removal of Various Pollutants from Water and Wastewater by Modified Chitosan Adsorbents. *Crit. Rev. Environ. Sci. Technol.* **2017**, *47*, 2331–2386. [CrossRef]
28. Wang, G.; Liu, J.; Wang, X.; Xie, Z.; Deng, N. Adsorption of Uranium (VI) from Aqueous Solution onto Cross-Linked Chitosan. *J. Hazard. Mater.* **2009**, *168*, 1053–1058. [CrossRef] [PubMed]
29. Galamboš, M.; Suchánek, P.; Rosskopfová, O. Sorption of Anthropogenic Radionuclides on Natural and Synthetic Inorganic Sorbents. *J. Radioanal. Nucl. Chem.* **2012**, *293*, 613–633. [CrossRef]
30. Means, J.L.; Crerar, D.A.; Borcsik, M.P.; Duguid, J.O. Radionuclide Adsorption by Manganese Oxides and Implications for Radioactive Waste Disposal. *Nature* **1978**, *274*, 44–47. [CrossRef]
31. Musić, S.; Ristić, M. Adsorption of Trace Elements or Radionuclides on Hydrous Iron Oxides. *J. Radioanal. Nucl. Chem.* **1988**, *120*, 289–304. [CrossRef]
32. Lu, S.; Sun, Y.; Chen, C. Adsorption of Radionuclides on Carbon-Based Nanomaterials. In *Interface Science and Technology*; Elsevier: Amsterdam, The Netherlands, 2019; Volume 29, pp. 141–215.
33. Claverie, M.; Garcia, J.; Prevost, T.; Brendlé, J.; Limousy, L. Inorganic and Hybrid (Organic–Inorganic) Lamellar Materials for Heavy Metals and Radionuclides Capture in Energy Wastes Management—A Review. *Materials* **2019**, *12*, 1399. [CrossRef] [PubMed]
34. Naeimi, S.; Faghihian, H. Performance of Novel Adsorbent Prepared by Magnetic Metal-Organic Framework (MOF) Modified by Potassium Nickel Hexacyanoferrate for Removal of Cs+ from Aqueous Solution. *Sep. Purif. Technol.* **2017**, *175*, 255–265. [CrossRef]
35. Sun, Q.; Aguila, B.; Ma, S. Opportunities of Porous Organic Polymers for Radionuclide Sequestration. *Trends Chem.* **2019**, *1*, 292–303. [CrossRef]
36. Vellingiri, K.; Kim, K.-H.; Pournara, A.; Deep, A. Towards High-Efficiency Sorptive Capture of Radionuclides in Solution and Gas. *Prog. Mater. Sci.* **2018**, *94*, 1–67. [CrossRef]
37. Chen, L.; Xu, S.; Li, J. Recent Advances in Molecular Imprinting Technology: Current Status, Challenges and Highlighted Applications. *Chem. Soc. Rev.* **2011**, *40*, 2922–2942. [CrossRef] [PubMed]
38. Haupt, K. Imprinted Polymers—Tailor-Made Mimics of Antibodies and Receptors. *Chem. Commun.* **2003**, 171–178. [CrossRef] [PubMed]
39. Tarley, C.R.T.; Corazza, M.Z.; Somera, B.F.; Segatelli, M.G. Preparation of New Ion-Selective Cross-Linked Poly (Vinylimidazole-Co-Ethylene Glycol Dimethacrylate) Using a Double-Imprinting Process for the Preconcentration of Pb2+ Ions. *J. Colloid Interface Sci.* **2015**, *450*, 254–263. [CrossRef] [PubMed]
40. Mahony, J.O.; Nolan, K.; Smyth, M.R.; Mizaikoff, B. Molecularly Imprinted Polymers—Potential and Challenges in Analytical Chemistry. *Anal. Chim. Acta* **2005**, *534*, 31–39. [CrossRef]
41. Rao, T.P.; Daniel, S.; Gladis, J.M. Tailored Materials for Preconcentration or Separation of Metals by Ion-Imprinted Polymers for Solid-Phase Extraction (IIP-SPE). *TrAC Trends Anal. Chem.* **2004**, *23*, 28–35.
42. Wulff, G. Molecular Imprinting in Cross-linked Materials with the Aid of Molecular Templates—A Way towards Artificial Antibodies. *Angew. Chem. Int. Ed. Engl.* **1995**, *34*, 1812–1832. [CrossRef]
43. Haupt, K.; Mosbach, K. Molecularly Imprinted Polymers and Their Use in Biomimetic Sensors. *Chem. Rev.* **2000**, *100*, 2495–2504. [CrossRef]
44. Fu, J.; Chen, L.; Li, J.; Zhang, Z. Current Status and Challenges of Ion Imprinting. *J. Mater. Chem. A* **2015**, *3*, 13598–13627. [CrossRef]
45. Metilda, P.; Gladis, J.M.; Rao, T.P. Influence of Binary/Ternary Complex of Imprint Ion on the Preconcentration of Uranium (VI) Using Ion Imprinted Polymer Materials. *Anal. Chim. Acta* **2004**, *512*, 63–73. [CrossRef]
46. Nishide, H.; Deguchi, J.; Tsuchida, E. Selective Adsorption of Metal Ions on Crosslinked Poly (Vinylpyridine) Resin Prepared with a Metal Ion as a Template. *Chem. Lett.* **1976**, *5*, 169–174. [CrossRef]
47. Saunders, G.D.; Foxon, S.P.; Walton, P.H.; Joyce, M.J.; Port, S.N. A Selective Uranium Extraction Agent Prepared by Polymer ImprintingS. N. Port, MJ Joyce, PH Walton and GD Saunders, UK Pat. Appl., 979946.7, 1997; Int. Pat., WO 99/15707, 1998. *Chem. Commun.* **2000**, 273–274. [CrossRef]
48. He, Q.; Chang, X.; Wu, Q.; Huang, X.; Hu, Z.; Zhai, Y. Synthesis and Applications of Surface-Grafted Th (IV)-Imprinted Polymers for Selective Solid-Phase Extraction of Thorium (IV). *Anal. Chim. Acta* **2007**, *605*, 192–197. [CrossRef] [PubMed]
49. Mafu, L.D.; Msagati, T.A.M.; Mamba, B.B. Ion-Imprinted Polymers for Environmental Monitoring of Inorganic Pollutants: Synthesis, Characterization, and Applications. *Environ. Sci. Pollut. Res.* **2013**, *20*, 790–802. [CrossRef]
50. Hande, P.E.; Samui, A.B.; Kulkarni, P.S. Highly Selective Monitoring of Metals by Using Ion-Imprinted Polymers. *Environ. Sci. Pollut. Res.* **2015**, *22*, 7375–7404. [CrossRef]
51. Branger, C.; Meouche, W.; Margaillan, A. Recent Advances on Ion-Imprinted Polymers. *React. Funct. Polym.* **2013**, *73*, 859–875. [CrossRef]

52. He, M.F.A.R.H.; Brada, S.T.M. A Mini Review on Molecularly Imprinted Polymer Based Halloysite Nanotubes Composites: Innovative Materials for Analytical and Environmental Applications. *Rev. Environ. Sci. Bio/Technol.* **2020**, *19*, 241–258.
53. Erdem, Ö.; Saylan, Y.; Andaç, M.; Denizli, A. Molecularly Imprinted Polymers for Removal of Metal Ions: An Alternative Treatment Method. *Biomimetics* **2018**, *3*, 38. [CrossRef] [PubMed]
54. Chen, L.; Dai, J.; Hu, B.; Wang, J.; Wu, Y.; Dai, J.; Meng, M.; Li, C.; Yan, Y. Recent Progresses on the Adsorption and Separation of Ions by Imprinting Routes. *Sep. Purif. Rev.* **2019**, *49*, 268–293. [CrossRef]
55. Say, R.; Birlik, E.; Ersöz, A.; Yılmaz, F.; Gedikbey, T.; Denizli, A. Preconcentration of Copper on Ion-Selective Imprinted Polymer Microbeads. *Anal. Chim. Acta* **2003**, *480*, 251–258. [CrossRef]
56. Nicholls, I.A.; Adbo, K.; Andersson, H.S.; Andersson, P.O.; Ankarloo, J.; Hedin-Dahlström, J.; Jokela, P.; Karlsson, J.G.; Olofsson, L.; Rosengren, J.; et al. Can We Rationally Design Molecularly Imprinted Polymers? *Anal. Chim. Acta* **2001**, *435*, 9–18. [CrossRef]
57. Laatikainen, K.; Udomsap, D.; Siren, H.; Brisset, H.; Sainio, T.; Branger, C. Effect of Template Ion–Ligand Complex Stoichiometry on Selectivity of Ion-Imprinted Polymers. *Talanta* **2015**, *134*, 538–545. [CrossRef] [PubMed]
58. Özkara, S.; Andaç, M.; Karakoç, V.; Say, R.; Denizli, A. Ion-imprinted PHEMA Based Monolith for the Removal of Fe3+ Ions from Aqueous Solutions. *J. Appl. Polym. Sci.* **2011**, *120*, 1829–1836. [CrossRef]
59. Sharma, G.; Kandasubramanian, B. Molecularly Imprinted Polymers for Selective Recognition and Extraction of Heavy Metal Ions and Toxic Dyes. *J. Chem. Eng. Data* **2020**, *65*, 396–418. [CrossRef]
60. Meng, H.; Li, Z.; Ma, F.; Jia, L.; Wang, X.; Zhou, W.; Zhang, L. Preparation and Characterization of Surface Imprinted Polymer for Selective Sorption of Uranium (VI). *J. Radioanal. Nucl. Chem.* **2015**, *306*, 139–146. [CrossRef]
61. Germiniano, T.O.; Corazza, M.Z.; Segatelli, M.G.; Ribeiro, E.S.; Yabe, M.J.S.; Galunin, E.; Tarley, C.R.T. Synthesis of Novel Copper Ion-Selective Material Based on Hierarchically Imprinted Cross-Linked Poly (Acrylamide-Co-Ethylene Glycol Dimethacrylate). *React. Funct. Polym.* **2014**, *82*, 72–80. [CrossRef]
62. Mafu, L.D.; Mamba, B.B.; Msagati, T.A.M. Synthesis and Characterization of Ion Imprinted Polymeric Adsorbents for the Selective Recognition and Removal of Arsenic and Selenium in Wastewater Samples. *J. Saudi Chem. Soc.* **2016**, *20*, 594–605. [CrossRef]
63. Cai, X.; Li, J.; Zhang, Z.; Yang, F.; Dong, R.; Chen, L. Novel Pb2+ Ion Imprinted Polymers Based on Ionic Interaction via Synergy of Dual Functional Monomers for Selective Solid-Phase Extraction of Pb2+ in Water Samples. *ACS Appl. Mater. Interfaces* **2014**, *6*, 305–313. [CrossRef] [PubMed]
64. Rodríguez-Fernández, R.; Peña-Vázquez, E.; Bermejo-Barrera, P. Synthesis of an Imprinted Polymer for the Determination of Methylmercury in Marine Products. *Talanta* **2015**, *144*, 636–641. [CrossRef] [PubMed]
65. Jinadasa, K.K.; Peña-Vázquez, E.; Bermejo-Barrera, P.; Moreda-Piñeiro, A. Ionic Imprinted Polymer Solid-Phase Extraction for Inorganic Arsenic Selective Pre-Concentration in Fishery Products before High-Performance Liquid Chromatography–Inductively Coupled Plasma-Mass Spectrometry Speciation. *J. Chromatogr. A* **2020**, *1619*, 460973. [CrossRef] [PubMed]
66. Yordanova, T.; Dakova, I.; Balashev, K.; Karadjova, I. Polymeric Ion-Imprinted Nanoparticles for Mercury Speciation in Surface Waters. *Microchem. J.* **2014**, *113*, 42–47. [CrossRef]
67. Anirudhan, T.S.; Nima, J.; Divya, P.L. Adsorption and Separation Behavior of Uranium (VI) by 4-Vinylpyridine-Grafted-Vinyltriethoxysilane-Cellulose Ion Imprinted Polymer. *J. Environ. Chem. Eng.* **2015**, *3*, 1267–1276. [CrossRef]
68. Comba, P.; Schiek, W. Fit and Misfit between Ligands and Metal Ions. *Coord. Chem. Rev.* **2003**, *238*, 21–29. [CrossRef]
69. Fasihi, J.; Alahyari, S.A.; Shamsipur, M.; Sharghi, H.; Charkhi, A. Adsorption of Uranyl Ion onto an Anthraquinone Based Ion-Imprinted Copolymer. *React. Funct. Polym.* **2011**, *71*, 803–808. [CrossRef]
70. Zulfikar, M.A.; Zarlina, R.; Handayani, N.; Alni, A.; Wahyuningrum, D. Separation of Yttrium from Aqueous Solution Using Ionic Imprinted Polymers. *Russ. J. Non-Ferrous Met.* **2017**, *58*, 614–624. [CrossRef]
71. Muzzarelli, R.A.A. Potential of Chitin/Chitosan-Bearing Materials for Uranium Recovery: An Interdisciplinary Review. *Carbohydr. Polym.* **2011**, *84*, 54–63. [CrossRef]
72. Monier, M.; Abdel-Latif, D.A.; Mohammed, H.A. Synthesis and Characterization of Uranyl Ion-Imprinted Microspheres Based on Amidoximated Modified Alginate. *Int. J. Biol. Macromol.* **2015**, *75*, 354–363. [CrossRef] [PubMed]
73. Ngah, W.S.W.; Teong, L.C.; Hanafiah, M.A.K.M. Adsorption of Dyes and Heavy Metal Ions by Chitosan Composites: A Review. *Carbohydr. Polym.* **2011**, *83*, 1446–1456. [CrossRef]
74. Özkahraman, B.; Özbaş, Z.; Öztürk, A.B. Synthesis of Ion-Imprinted Alginate Based Beads: Selective Adsorption Behavior of Nickel (II) Ions. *J. Polym. Environ.* **2018**, *26*, 4303–4310. [CrossRef]
75. Okay, O. Macroporous Copolymer Networks. *Prog. Polym. Sci.* **2000**, *25*, 711–779. [CrossRef]
76. Yoshizako, K.; Hosoya, K.; Iwakoshi, Y.; Kimata, K.; Tanaka, N. Porogen Imprinting Effects. *Anal. Chem.* **1998**, *70*, 386–389. [CrossRef]
77. Rammika, M.; Darko, G.; Torto, N. Optimal Synthesis of a Ni (II)-Dimethylglyoxime Ion-Imprinted Polymer for the Enrichment of Ni (II) Ions in Water, Soil and Mine Tailing Samples. *Water SA* **2012**, *38*, 261–268. [CrossRef]
78. Lin, C.; Wang, H.; Wang, Y.; Zhou, L.; Liang, J. Selective Preconcentration of Trace Thorium from Aqueous Solutions with Th (IV)-Imprinted Polymers Prepared by a Surface-Grafted Technique. *Int. J. Environ. Anal. Chem.* **2011**, *91*, 1050–1061. [CrossRef]
79. Monier, M.; Abdel-Latif, D.A. Synthesis and Characterization of Ion-Imprinted Resin Based on Carboxymethyl Cellulose for Selective Removal of UO22+. *Carbohydr. Polym.* **2013**, *97*, 743–752. [CrossRef]
80. Ji, X.Z.; Liu, H.J.; Wang, L.L.; Sun, Y.K.; Wu, Y.W. Study on Adsorption of Th (IV) Using Surface Modified Dibenzoylmethane Molecular Imprinted Polymer. *J. Radioanal. Nucl. Chem.* **2013**, *295*, 265–270. [CrossRef]

81. Chen, J.; Bai, H.; Xia, J.; Liu, X.; Liu, Y. Trace Detection of Ce3+ by Adsorption Strip Voltammetry at a Carbon Paste Electrode Modified with Ion Imprinted Polymers. *J. Rare Earths* **2018**, *36*, 1121–1126. [CrossRef]
82. Liu, Y.; Meng, X.; Luo, M.; Meng, M.; Ni, L.; Qiu, J.; Hu, Z.; Liu, F.; Zhong, G.; Liu, Z. Synthesis of Hydrophilic Surface Ion-Imprinted Polymer Based on Graphene Oxide for Removal of Strontium from Aqueous Solution. *J. Mater. Chem. A* **2015**, *3*, 1287–1297. [CrossRef]
83. Salian, V.D.; Byrne, M.E. Living Radical Polymerization and Molecular Imprinting: Improving Polymer Morphology in Imprinted Polymers. *Macromol. Mater. Eng.* **2013**, *298*, 379–390. [CrossRef]
84. Chen, Y.; Wang, J. Removal of Radionuclide Sr2+ Ions from Aqueous Solution Using Synthesized Magnetic Chitosan Beads. *Nucl. Eng. Des.* **2012**, *242*, 445–451. [CrossRef]
85. Gao, M.; Zhu, G.; Gao, C. A Review: Adsorption Materials for the Removal and Recovery of Uranium from Aqueous Solutions. *Energy Environ. Focus* **2014**, *3*, 219–226. [CrossRef]
86. Gao, D.; Zhang, Z.; Wu, M.; Xie, C.; Guan, G.; Wang, D. A Surface Functional Monomer-Directing Strategy for Highly Dense Imprinting of TNT at Surface of Silica Nanoparticles. *J. Am. Chem. Soc.* **2007**, *129*, 7859–7866. [CrossRef]
87. Volesky, B. *Sorption and Biosorption*; BV Sorbex, Inc.: Montreal, QC, Canada, 2003; pp. 103–116.
88. Wang, J.; Guo, X. Adsorption Isotherm Models: Classification, Physical Meaning, Application and Solving Method. *Chemosphere* **2020**, *258*, 127279. [CrossRef] [PubMed]
89. Cheng, Z.; Wang, H.; Wang, Y.; He, F.; Zhang, H.; Yang, S. Synthesis and Characterization of an Ion-Imprinted Polymer for Selective Solid Phase Extraction of Thorium (IV). *Microchim. Acta* **2011**, *173*, 423–431. [CrossRef]
90. Tavengwa, N.T.; Cukrowska, E.; Chimuka, L. Sequestration of U (VI) from Aqueous Solutions Using Precipitate Ion Imprinted Polymers Endowed with Oleic Acid Functionalized Magnetite. *J. Radioanal. Nucl. Chem.* **2015**, *304*, 933–943. [CrossRef]
91. Meng, X.; Liu, Y.; Meng, M.; Gu, Z.; Ni, L.; Zhong, G.; Liu, F.; Hu, Z.; Chen, R.; Yan, Y. Synthesis of Novel Ion-Imprinted Polymers by Two Different RAFT Polymerization Strategies for the Removal of Cs (I) from Aqueous Solutions. *RSC Adv.* **2015**, *5*, 12517–12529. [CrossRef]
92. Sadeghi, S.; Aboobakri, E. Magnetic Nanoparticles with an Imprinted Polymer Coating for the Selective Extraction of Uranyl Ions. *Microchim. Acta* **2012**, *178*, 89–97. [CrossRef]
93. Liu, F.; Liu, Y.; Xu, Y.; Ni, L.; Meng, X.; Hu, Z.; Zhong, G.; Meng, M.; Wang, Y.; Han, J. Efficient Static and Dynamic Removal of Sr (II) from Aqueous Solution Using Chitosan Ion-Imprinted Polymer Functionalized with Dithiocarbamate. *J. Environ. Chem. Eng.* **2015**, *3*, 1061–1071. [CrossRef]
94. Song, Y.; Ou, H.; Bian, W.; Zhang, Y.; Pan, J.; Liu, Y.; Huang, W. Ion-Imprinted Polymers Based on Hollow Silica with Yeasts as Sacrificial Supports for Sr 2+ Selective Adsorption. *J. Inorg. Organomet. Polym. Mater.* **2013**, *23*, 1325–1334. [CrossRef]
95. Kang, R.; Qiu, L.; Fang, L.; Yu, R.; Chen, Y.; Lu, X.; Luo, X. A Novel Magnetic and Hydrophilic Ion-Imprinted Polymer as a Selective Sorbent for the Removal of Cobalt Ions from Industrial Wastewater. *J. Environ. Chem. Eng.* **2016**, *4*, 2268–2277. [CrossRef]
96. Shu, X.; Shen, L.; Wei, Y.; Hua, D. Synthesis of Surface Ion-Imprinted Magnetic Microsphere for Efficient Sorption of Perrhenate: A Structural Surrogate for Pertechnetate. *J. Mol. Liq.* **2015**, *211*, 621–627. [CrossRef]
97. Tavengwa, N.T.; Cukrowska, E.; Chimuka, L. Synthesis of Bulk Ion-Imprinted Polymers (IIPs) Embedded with Oleic Acid Coated Fe 3 O 4 for Selective Extraction of Hexavalent Uranium. *Water SA* **2014**, *40*, 623–630. [CrossRef]
98. Aly, M.M.; Hamza, M.F. A Review: Studies on Uranium Removal Using Different Techniques. Overview. *J. Dispers. Sci. Technol.* **2013**, *34*, 182–213. [CrossRef]
99. Ahmadi, S.J.; Noori-Kalkhoran, O.; Shirvani-Arani, S. Synthesis and Characterization of New Ion-Imprinted Polymer for Separation and Preconcentration of Uranyl (UO22+) Ions. *J. Hazard. Mater.* **2010**, *175*, 193–197. [CrossRef]
100. Milja, T.E.; Prathish, K.P.; Rao, T.P. Synthesis of Surface Imprinted Nanospheres for Selective Removal of Uranium from Simulants of Sambhar Salt Lake and Ground Water. *J. Hazard. Mater.* **2011**, *188*, 384–390. [CrossRef]
101. Liu, Y.; Cao, X.; Hua, R.; Wang, Y.; Liu, Y.; Pang, C.; Wang, Y. Selective Adsorption of Uranyl Ion on Ion-Imprinted Chitosan/PVA Cross-Linked Hydrogel. *Hydrometallurgy* **2010**, *104*, 150–155. [CrossRef]
102. Zhou, L.; Shang, C.; Liu, Z.; Huang, G.; Adesina, A.A. Selective Adsorption of Uranium (VI) from Aqueous Solutions Using the Ion-Imprinted Magnetic Chitosan Resins. *J. Colloid Interface Sci.* **2012**, *366*, 165–172. [CrossRef]
103. Yang, S.; Qian, J.; Kuang, L.; Hua, D. Ion-Imprinted Mesoporous Silica for Selective Removal of Uranium from Highly Acidic and Radioactive Effluent. *ACS Appl. Mater. Interfaces* **2017**, *9*, 29337–29344. [CrossRef] [PubMed]
104. Zhu, J.; Liu, Q.; Liu, J.; Chen, R.; Zhang, H.; Yu, J.; Zhang, M.; Li, R.; Wang, J. Novel Ion-Imprinted Carbon Material Induced by Hyperaccumulation Pathway for the Selective Capture of Uranium. *ACS Appl. Mater. Interfaces* **2018**, *10*, 28877–28886. [CrossRef]
105. Wang, Z.; Zhang, D.; Xiao, X.; Su, C.; Li, Z.; Xue, J.; Hu, N.; Peng, P.; Liao, L.; Wang, H. A Highly Sensitive and Selective Sensor for Trace Uranyl (VI) Ion Based on a Graphene-Coated Carbon Paste Electrode Modified with Ion Imprinted Polymer. *Microchem. J.* **2020**, *155*, 104767. [CrossRef]
106. Zhong, X.; Sun, Y.; Zhang, Z.; Dai, Y.; Wang, Y.; Liu, Y.; Hua, R.; Cao, X.; Liu, Y. A New Hydrothermal Cross-Linking Ion-Imprinted Chitosan for High-Efficiency Uranium Removal. *J. Radioanal. Nucl. Chem.* **2019**, *322*, 901–911. [CrossRef]
107. Zhang, H.; Liang, H.; Chen, Q.; Shen, X. Synthesis of a New Ionic Imprinted Polymer for the Extraction of Uranium from Seawater. *J. Radioanal. Nucl. Chem.* **2013**, *298*, 1705–1712. [CrossRef]

108. Tavengwa, N.T.; Cukrowska, E.; Chimuka, L. Preparation, Characterization and Application of $NaHCO_3$ Leached Bulk U (VI) Imprinted Polymers Endowed with γ-MPS Coated Magnetite in Contaminated Water. *J. Hazard. Mater.* **2014**, *267*, 221–228. [CrossRef]
109. Monier, M.; Elsayed, N.H. Selective Extraction of Uranyl Ions Using Ion-Imprinted Chelating Microspheres. *J. Colloid Interface Sci.* **2014**, *423*, 113–122. [CrossRef] [PubMed]
110. Güney, S.; Güney, O. A Novel Electrochemical Sensor for Selective Determination of Uranyl Ion Based on Imprinted Polymer Sol–Gel Modified Carbon Paste Electrode. *Sens. Actuators B Chem.* **2016**, *231*, 45–53. [CrossRef]
111. Arnold, J.; Gianetti, T.L.; Kashtan, Y. Thorium Lends a Fiery Hand. *Nat. Chem.* **2014**, *6*, 554. [CrossRef]
112. Lin, C.; Wang, H.; Wang, Y.; Cheng, Z. Selective Solid-Phase Extraction of Trace Thorium (IV) Using Surface-Grafted Th (IV)-Imprinted Polymers with Pyrazole Derivative. *Talanta* **2010**, *81*, 30–36. [CrossRef]
113. He, F.F.; Wang, H.Q.; Wang, Y.Y.; Wang, X.F.; Zhang, H.S.; Li, H.L.; Tang, J.H. Magnetic Th (IV)-Ion Imprinted Polymers with Salophen Schiff Base for Separation and Recognition of Th (IV). *J. Radioanal. Nucl. Chem.* **2013**, *295*, 167–177. [CrossRef]
114. Huang, G.; Chen, Z.; Wang, L.; Lv, T.; Shi, J. Removal of Thorium (IV) from Aqueous Solution Using Magnetic Ion-Imprinted Chitosan Resin. *J. Radioanal. Nucl. Chem.* **2016**, *310*, 1265–1272. [CrossRef]
115. Othman, N.A.F.; Selambakkannu, S.; Azian, H.; Ratnam, C.T.; Yamanobe, T.; Hoshina, H.; Seko, N. Synthesis of Surface Ion-Imprinted Polymer for Specific Detection of Thorium under Acidic Conditions. *Polym. Bull.* **2020**, *78*, 165–183. [CrossRef]
116. Khandaker, S.; Chowdhury, M.F.; Awual, M.R.; Islam, A.; Kuba, T. Efficient Cesium Encapsulation from Contaminated Water by Cellulosic Biomass Based Activated Wood Charcoal. *Chemosphere* **2020**, *262*, 127801. [CrossRef] [PubMed]
117. Alby, D.; Charnay, C.; Heran, M.; Prelot, B.; Zajac, J. Recent Developments in Nanostructured Inorganic Materials for Sorption of Cesium and Strontium: Synthesis and Shaping, Sorption Capacity, Mechanisms, and Selectivity—A Review. *J. Hazard. Mater.* **2018**, *344*, 511–530. [CrossRef] [PubMed]
118. Zhang, Z.; Xu, X.; Yan, Y. Kinetic and Thermodynamic Analysis of Selective Adsorption of Cs (I) by a Novel Surface Whisker-Supported Ion-Imprinted Polymer. *Desalination* **2010**, *263*, 97–106. [CrossRef]
119. Shamsipur, M.; Rajabi, H.R. Flame Photometric Determination of Cesium Ion after Its Preconcentration with Nanoparticles Imprinted with the Cesium-Dibenzo-24-Crown-8 Complex. *Microchim. Acta* **2013**, *180*, 243–252. [CrossRef]
120. Iwasaki, H.; Yoshikawa, M. Molecularly Imprinted Polyacrylonitrile Adsorbents for the Capture of Cs+ Ions. *Polym. J.* **2016**, *48*, 1151–1156. [CrossRef]
121. Burger, A.; Lichtscheidl, I. Strontium in the Environment: Review about Reactions of Plants towards Stable and Radioactive Strontium Isotopes. *Sci. Total Environ.* **2019**, *653*, 1458–1512. [CrossRef] [PubMed]
122. Liu, Y.; Gao, J.; Zhang, Z.; Dai, J.; Xie, J.; Yan, Y. A New Sr (II) Ion-Imprinted Polymer Grafted onto Potassium Titanate Whiskers: Synthesis and Adsorption Performance for the Selective Separation of Strontium Ions. *Adsorpt. Sci. Technol.* **2010**, *28*, 23–37. [CrossRef]
123. Bahraini, N.; Lai, E.P.C.; Li, C.; Sadi, B.B.; Kramer, G.H. Molecularly Imprinted Polymers for 90Sr Urine Bioassay. *Health Phys.* **2011**, *101*, 128–135. [CrossRef] [PubMed]
124. Pan, J.; Zou, X.; Yan, Y.; Wang, X.; Guan, W.; Han, J.; Wu, X. An Ion-Imprinted Polymer Based on Palygorskite as a Sacrificial Support for Selective Removal of Strontium (II). *Appl. Clay Sci.* **2010**, *50*, 260–265. [CrossRef]
125. Liu, Y.; Chen, R.; Yuan, D.; Liu, Z.; Meng, M.; Wang, Y.; Han, J.; Meng, X.; Liu, F.; Hu, Z. Thermal-Responsive Ion-Imprinted Polymer Based on Magnetic Mesoporous Silica SBA-15 for Selective Removal of Sr (II) from Aqueous Solution. *Colloid Polym. Sci.* **2015**, *293*, 109–123. [CrossRef]
126. Liu, Y.; Liu, F.; Ni, L.; Meng, M.; Meng, X.; Zhong, G.; Qiu, J. A Modeling Study by Response Surface Methodology (RSM) on Sr (II) Ion Dynamic Adsorption Optimization Using a Novel Magnetic Ion Imprinted Polymer. *RSC Adv.* **2016**, *6*, 54679–54692. [CrossRef]
127. Wapstra, A.H.; Thibault, C.; Blachot, J.; Bersillon, O. The NUBASE Evaluation of Nuclear and Decay Properties G. Audi. *Nucl. Phys. A* **2003**, *729*, 3–128.
128. Pan, J.; Zou, X.; Li, C.; Liu, Y.; Yan, Y.; Han, J. Synthesis and Applications of Ce (III)-Imprinted Polymer Based on Attapulgite as the Sacrificial Support Material for Selective Separation of Cerium (III) Ions. *Microchim. Acta* **2010**, *171*, 151–160. [CrossRef]
129. Zhang, X.; Li, C.; Yan, Y.; Pan, J.; Xu, P.; Zhao, X. A Ce 3+-Imprinted Functionalized Potassium Tetratitanate Whisker Sorbent Prepared by Surface Molecularly Imprinting Technique for Selective Separation and Determination of Ce 3+. *Microchim. Acta* **2010**, *169*, 289–296. [CrossRef]
130. Prasad, B.B.; Jauhari, D. Double-Ion Imprinted Polymer@ Magnetic Nanoparticles Modified Screen Printed Carbon Electrode for Simultaneous Analysis of Cerium and Gadolinium Ions. *Anal. Chim. Acta* **2015**, *875*, 83–91. [CrossRef]
131. Alizadeh, T.; Ganjali, M.R.; Akhoundian, M.; Norouzi, P. Voltammetric Determination of Ultratrace Levels of Cerium (III) Using a Carbon Paste Electrode Modified with Nano-Sized Cerium-Imprinted Polymer and Multiwalled Carbon Nanotubes. *Microchim. Acta* **2016**, *183*, 1123–1130. [CrossRef]
132. Keçili, R.; Dolak, İ.; Ziyadanoğulları, B.; Ersöz, A.; Say, R. Ion Imprinted Cryogel-Based Supermacroporous Traps for Selective Separation of Cerium (III) in Real Samples. *J. Rare Earths* **2018**, *36*, 857–862. [CrossRef]
133. Liu, Y.; Tian, S.; Meng, X.; Dai, X.; Liu, Z.; Meng, M.; Han, J.; Wang, Y.; Chen, R.; Yan, Y. Synthesis, Characterization, and Adsorption Properties of a Ce (III)-Imprinted Polymer Supported by Mesoporous SBA-15 Matrix by a Surface Molecular Imprinting Technique. *Can. J. Chem.* **2014**, *92*, 257–266. [CrossRef]

134. Daňo, M.; Viglašová, E.; Galamboš, M.; Štamberg, K.; Kujan, J. Surface Complexation Models of Pertechnetate on Biochar/Montmorillonite Composite—Batch and Dynamic Sorption Study. *Materials* **2020**, *13*, 3108. [CrossRef] [PubMed]
135. Sert, Ş.; Kütahyali, C.; İnan, S.; Talip, Z.; Çetinkaya, B.; Eral, M. Biosorption of Lanthanum and Cerium from Aqueous Solutions by Platanus Orientalis Leaf Powder. *Hydrometallurgy* **2008**, *90*, 13–18. [CrossRef]
136. Wang, J.; Wei, J.; Li, J. Straw-Supported Ion Imprinted Polymer Sorbent Prepared by Surface Imprinting Technique Combined with AGET ATRP for Selective Adsorption of La3+ Ions. *Chem. Eng. J.* **2016**, *293*, 24–33. [CrossRef]
137. Nik Mustapa, N.R.; Malek, N.F.A.; Yusoff, M.M.; Rahman, M.L. Ion Imprinted Polymers for Selective Recognition and Separation of Lanthanum and Cerium Ions from Other Lanthanide. *Sep. Sci. Technol.* **2016**, *51*, 2762–2771. [CrossRef]
138. Besharati-Seidani, A.; Shamsipur, M. Ion-Imprinted Polymeric Nanoparticles for Fast and Selective Separation of Lanthanum (III). *Microchim. Acta* **2015**, *182*, 1747–1755. [CrossRef]
139. Trzonkowska, L.; Leśniewska, B.; Godlewska-Żyłkiewicz, B. Studies on the Effect of Functional Monomer and Porogen on the Properties of Ion Imprinted Polymers Based on Cr (III)-1, 10-Phenanthroline Complex Designed for Selective Removal of Cr (III) Ions. *React. Funct. Polym.* **2017**, *117*, 131–139. [CrossRef]
140. Liang, Q.; Geng, J.; Luo, H.; Fang, W.; Yin, Y. Fast and Selective Removal of Cr (VI) from Aqueous Solutions by a Novel Magnetic Cr (VI) Ion-Imprinted Polymer. *J. Mol. Liq.* **2017**, *248*, 767–774. [CrossRef]
141. Zhou, Z.; Liu, X.; Zhang, M.; Jiao, J.; Zhang, H.; Du, J.; Zhang, B.; Ren, Z. Preparation of Highly Efficient Ion-Imprinted Polymers with Fe_3O_4 Nanoparticles as Carrier for Removal of Cr (VI) from Aqueous Solution. *Sci. Total Environ.* **2020**, *699*, 134334. [CrossRef]
142. Kumar, S.; Alveroğlu, E.; Balouch, A.; Talpur, F.N.; Jagirani, M.S.; Mahar, A.M.; Pato, A.H.; Mal, D.; Lal, S. Fabrication of Chromium-Imprinted Polymer: A Real Magneto-Selective Sorbent for the Removal of Cr (vi) Ions in Real Water Samples. *New J. Chem.* **2020**, *44*, 18668–18678. [CrossRef]
143. Zhou, Z.; Kong, D.; Zhu, H.; Wang, N.; Wang, Z.; Wang, Q.; Liu, W.; Li, Q.; Zhang, W.; Ren, Z. Preparation and Adsorption Characteristics of an Ion-Imprinted Polymer for Fast Removal of Ni (II) Ions from Aqueous Solution. *J. Hazard. Mater.* **2018**, *341*, 355–364. [CrossRef] [PubMed]
144. Ahmad, I.; Siddiqui, W.A.; Ahmad, T.; Siddiqui, V.U. Synthesis and Characterization of Molecularly Imprinted Ferrite (SiO_2@ Fe_2O_3) Nanomaterials for the Removal of Nickel (Ni2+ Ions) from Aqueous Solution. *J. Mater. Res. Technol.* **2019**, *8*, 1400–1411. [CrossRef]
145. Elsayed, N.; Alatawi, A.; Monier, M. Diacetylmonoxine Modified Chitosan Derived Ion-Imprinted Polymer for Selective Solid-Phase Extraction of Nickel (II) Ions. *React. Funct. Polym.* **2020**, *151*, 104570. [CrossRef]
146. Lenoble, V.; Laatikainen, K.; Garnier, C.; Angeletti, B.; Coulomb, B.; Sainio, T.; Branger, C. Nickel Retention by an Ion-Imprinted Polymer: Wide-Range Selectivity Study and Modelling of the Binding Structures. *Chem. Eng. J.* **2016**, *304*, 20–28. [CrossRef]
147. Leyssens, L.; Vinck, B.; Van Der Straeten, C.; Wuyts, F.; Maes, L. Cobalt Toxicity in Humans—A Review of the Potential Sources and Systemic Health Effects. *Toxicology* **2017**, *387*, 43–56. [CrossRef]
148. Su, Q.; Deng, L.; Ye, Q.; He, Y.; Cui, X. KOH-Activated Geopolymer Microspheres Recycle Co (II) with Higher Adsorption Capacity than NaOH-Activated Ones. *ACS Omega* **2020**, *5*, 23898–23908. [CrossRef]
149. Anirudhan, T.S.; Deepa, J.R.; Christa, J. Nanocellulose/Nanobentonite Composite Anchored with Multi-Carboxyl Functional Groups as an Adsorbent for the Effective Removal of Cobalt (II) from Nuclear Industry Wastewater Samples. *J. Colloid Interface Sci.* **2016**, *467*, 307–320. [CrossRef]
150. Liu, Y.; Gao, J.; Li, C.; Pan, J.; Yan, Y.; Xie, J. Synthesis and Adsorption Performance of Surface-Grafted Co (II)-Imprinted Polymer for Selective Removal of Cobalt. *Chin. J. Chem.* **2010**, *28*, 548–554. [CrossRef]
151. Li, C.; Pan, J.; Zou, X.; Gao, J.; Xie, J.; Yongsheng, Y. Synthesis and Applications of Novel Attapulgite-Supported Co (II)-Imprinted Polymers for Selective Solid-Phase Extraction of Cobalt (II) from Aqueous Solutions. *Int. J. Environ. Anal. Chem.* **2011**, *91*, 1035–1049. [CrossRef]
152. Liu, Y.; Liu, Z.; Dai, J.; Gao, J.; Xie, J.; Yan, Y. Selective Adsorption of Co (II) by Mesoporous Silica SBA-15-supported Surface Ion Imprinted Polymer: Kinetics, Isotherms, and Thermodynamics Studies. *Chin. J. Chem.* **2011**, *29*, 387–398. [CrossRef]
153. Pan, J.; Guan, W.; Zhang, Z.; Wang, X.; Li, C.; Yan, Y. Selective Adsorption of Co (II) Ions by Whisker Surface Ion-Imprinted Polymer: Equilibrium and Kinetics Modeling. *Chin. J. Chem.* **2010**, *28*, 2483–2488. [CrossRef]
154. Nishad, P.A.; Bhaskarapillai, A.; Velmurugan, S.; Narasimhan, S.V. Cobalt (II) Imprinted Chitosan for Selective Removal of Cobalt during Nuclear Reactor Decontamination. *Carbohydr. Polym.* **2012**, *87*, 2690–2696. [CrossRef]
155. Bhaskarapillai, A.; Narasimhan, S.V. A Comparative Investigation of Copper and Cobalt Imprinted Polymers: Evidence for Retention of the Solution-State Metal Ion–Ligand Complex Stoichiometry in the Imprinted Cavities. *RSC Adv.* **2013**, *3*, 13178–13182. [CrossRef]
156. Liu, F.B.; Jia, M.C.; Men, J.F.; Wang, X.W. Mn2+ and Co2+ Removal from Dilute Solution Using Cysteine Grafted Cobalt/Manganese Imprinted Crosslinked Chitosan. *Appl. Mech. Mater.* **2015**, *751*, 44–50. [CrossRef]
157. Turan, K.; Saygılı Canlıdinç, R.; Kalfa, O.M. Determination of Trace Amounts of Co (II) after Preconcentration with Surface Ion Imprinted Sorbent Based on Activated Carbon. *Sep. Sci. Technol.* **2018**, *53*, 707–716. [CrossRef]
158. Yuan, G.; Tu, H.; Liu, J.; Zhao, C.; Liao, J.; Yang, Y.; Yang, J.; Liu, N. A Novel Ion-Imprinted Polymer Induced by the Glycylglycine Modified Metal-Organic Framework for the Selective Removal of Co (II) from Aqueous Solutions. *Chem. Eng. J.* **2018**, *333*, 280–288. [CrossRef]

159. Torkashvand, M.; Gholivand, M.B.; Azizi, R. Synthesis, Characterization and Application of a Novel Ion-Imprinted Polymer Based Voltammetric Sensor for Selective Extraction and Trace Determination of Cobalt (II) Ions. *Sens. Actuators B Chem.* **2017**, *243*, 283–291. [CrossRef]
160. Sebastian, M.; Mathew, B. Multiwalled Carbon Nanotube Based Ion Imprinted Polymer as Sensor and Sorbent for Environmental Hazardous Cobalt Ion. *J. Macromol. Sci. Part A* **2018**, *55*, 455–465. [CrossRef]
161. Yusof, N.F.; Mehamod, F.S.; Suah, F.B.M. Fabrication and Binding Characterization of Ion Imprinted Polymers for Highly Selective Co2+ Ions in an Aqueous Medium. *J. Environ. Chem. Eng.* **2019**, *7*, 103007. [CrossRef]
162. Lee, V.E.; Schulman, J.M.; Stiefel, E.I.; Lee, C.C. Reversible Precipitation of Bovine Serum Albumin by Metal Ions and Synthesis, Structure and Reactivity of New Tetrathiometallate Chelating Agents. *J. Inorg. Biochem.* **2007**, *101*, 1707–1718. [CrossRef]
163. Li, S.; Li, J.; Ma, X.; Pang, C.; Yin, G.; Luo, J. Molecularly Imprinted Electroluminescence Switch Sensor with a Dual Recognition Effect for Determination of Ultra-Trace Levels of Cobalt (II). *Biosens. Bioelectron.* **2019**, *139*, 111321. [CrossRef] [PubMed]
164. Lee, H.-K.; Choi, J.-W.; Choi, S.-J. Magnetic Ion-Imprinted Polymer Based on Mesoporous Silica for Selective Removal of Co (II) from Radioactive Wastewater. *Sep. Sci. Technol.* **2020**, 1–11. [CrossRef]
165. Adibmehr, Z.; Faghihian, H. Preparation of Highly Selective Magnetic Cobalt Ion-Imprinted Polymer Based on Functionalized SBA-15 for Removal Co 2+ from Aqueous Solutions. *J. Environ. Health Sci. Eng.* **2019**, *17*, 1213–1225. [CrossRef]
166. Biswas, T.K.; Yusoff, M.M.; Sarjadi, M.S.; Arshad, S.E.; Musta, B.; Rahman, M.L. Ion-Imprinted Polymer for Selective Separation of Cobalt, Cadmium and Lead Ions from Aqueous Media. *Sep. Sci. Technol.* **2019**, 1–10. [CrossRef]